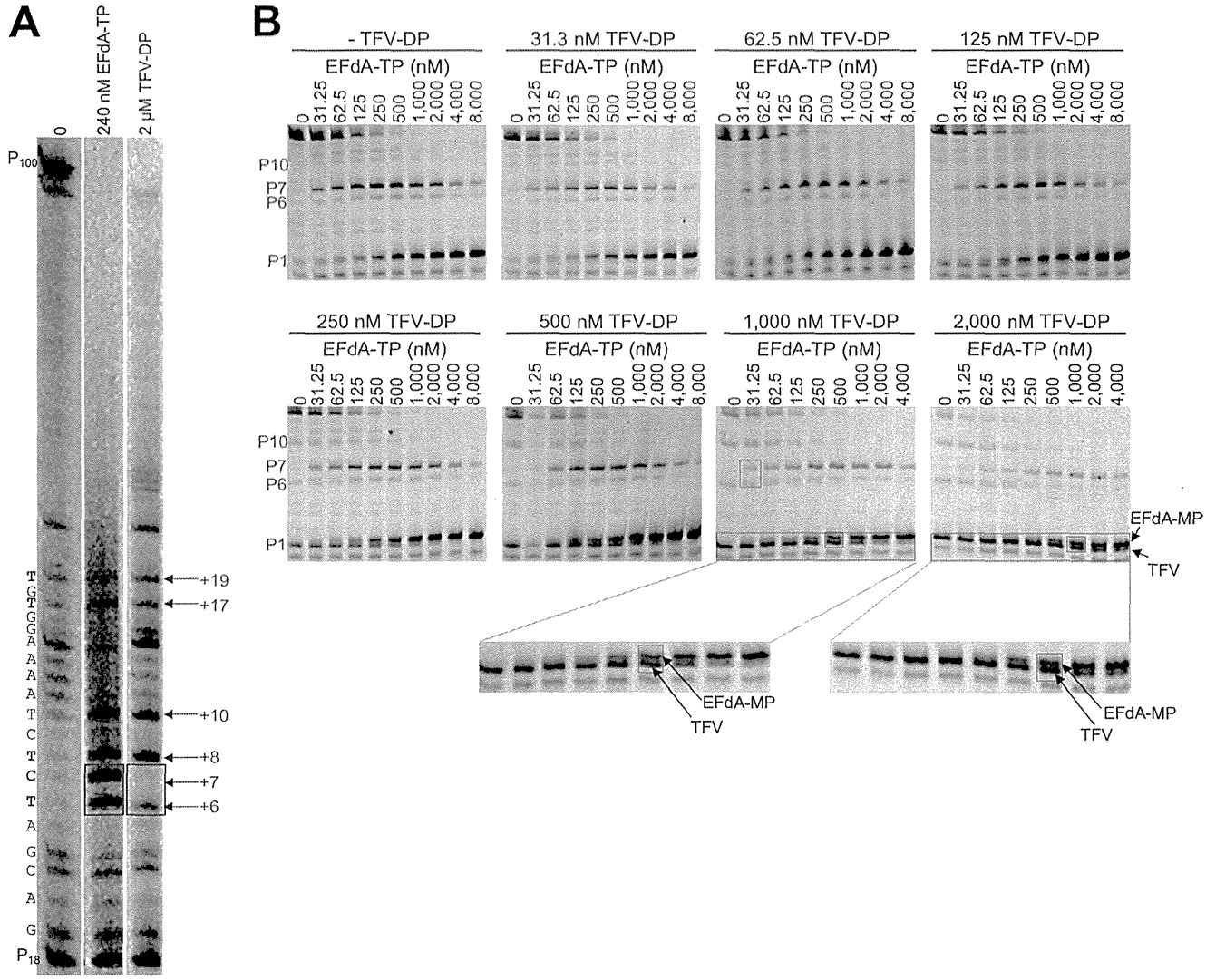

FIGURE 7. **EFdA-TP and TFV-DP have a different stopping pattern and do not always compete for the same incorporation sites.** *A*, using a long template, T_{d100}, we investigated the stopping pattern of EFdA-TP and TFV-DP. At some positions, both analogs appear to have similar incorporation efficiency (same intensity of bands). However, at position +6, EFdA-MP is incorporated more efficiently than TFV, or TFV is not incorporated at all (+7; DCT site). The sequence of template is shown next to the gels. *B*, $T_{d31(7C)}/P_{d18}$ (20 nM) was incubated with 20 nM RT for 15 min in the presence of 1 μM dNTPs, 6 mM $MgCl_2$, and various concentrations of EFdA-TP and TFV-DP. The sites where the inhibitors act as ICT or DCT are shown in *red* and *green*, respectively. In *red boxes*, we highlight some examples of ICT where both analogs are equally incorporated. In the *blue box*, we highlight the ICT and DCT sites at P6 and P7, respectively, where TFV and EFdA-MP, respectively, are equally incorporated.

TFV concentrations in Fig. 7*B*. Collectively, these data suggest that EFdA-TP and TFV-DP have different inhibition site specificities.

DISCUSSION

NRTIs were the first drugs used for the treatment of HIV infection and have always been part of first line antiretroviral therapies (1–8). All approved anti-HIV nucleoside analogs block RT-catalyzed DNA synthesis due to the lack of a 3′-OH group, which is necessary for DNA polymerization. Previously, we have shown that a series of 4′-substituted analogs with a 3′-OH possess anti-HIV activity (9–11). EFdA is the most potent of this series and, to our knowledge, the most potent NRTI with subnanomolar EC_{50} both in T-cells and peripheral blood mononuclear cells (10, 11, 16). The strong potency of EFdA is the result of its unique mechanism of action as well as its resistance to degradation by adenosine deaminase (15). Previously, we have reported that the inability of EFdA-MP-terminated primers to translocate from the N- to the P-site of HIV-1 RT causes inhibition of DNA polymerization (10). Here we demonstrate that EFdA inhibits RT with multiple mechanisms, which depend on the sequence of the nucleic acid substrate (Figs. 8 and 9).

There is a small number of reports on the effect of T/P sequence on RT inhibition by NRTIs. Scott and co-workers (43) reported that the primer terminus and adjacent upstream base pairs interact with HIV-1 RT in a sequence-dependent manner that affects the unblocking of NRTI-terminated primers. In addition, Hughes and co-workers (44) published that there is a difference in the extent of delayed chain termination by 4′-methyl dNTP analogs depending on the nucleic acid sequence. We report here that, depending on the T/P sequence, EFdA-TP can block RT either as a *de facto* ICT or as a DCT (Figs. 1, 2, 7, 8, and 9). Although EFdA-TP can inhibit RT both

as an ICT and a DCT, it appears that it predominantly inhibits at the point of incorporation (four of five sites in Fig. 7*A*), causing immediate chain termination and preventing enzyme translocation (Figs. 1, 8, and 9), thus acting as a translocation-defective RT inhibitor (10). Nonetheless, we have identified sites at various template sequences where EFdA-TP can also act as a DCT; it does not block enzyme translocation, allowing the incorporation of one additional dNTP before DNA synthesis is terminated.

What factors may lead to the differences in the mechanism of EFdA inhibition at the P1 (ICT) and P6-P7 (ICT and DCT) sites? We initially examined the effect of inhibitor incorporation efficiency as we anticipated that at sites of efficient EFdA-MP incorporation the EFdA-MP-terminated primer products ($T/P_{EFdA\text{-}MP}$) would be less likely to translocate, leading to immediate chain termination. Surprisingly, although EFdA-MP is better incorporated at the P6 site (Fig. 4), the footprinting experiments showed increased translocation at P6 (Fig. 1*C*), allowing more access to the dNTP-binding site and incorporation of the next complementary nucleotide ($T/P_{EFdA\text{-}MP\text{-}dNMP}$). Further polymerization may be inhibited by unfavorable interactions between the 4′-ethynyl of $T/P_{EFdA\text{-}MP\text{-}dNMP}$ and RT residues of the DNA-binding cleft.

We subsequently examined the effect of T/P sequence on the inhibition mechanism of EFdA. Our data definitively showed that a change of a single nucleotide can be sufficient to alter the inhibition mechanism from ICT to DCT (Fig. 2*A*, $T_{d31(5C)}/P_{d18}$ *versus* $T_{d31(5A)}/P_{d18}$), although in some cases, it does not have an effect (Fig. 2*B*, $T_{d31(4G5T)}/P_{d18}$ *versus* $T_{d31(4C5T)}/P_{d18}$). Hence, we conclude that the T/P sequence is a major factor that can determine the inhibition mechanism of EFdA. Ongoing structural studies are designed to determine the molecular basis for this specificity.

The ability of EFdA to inhibit RT with multiple mechanisms may have implications for current anti-HIV therapies. We recently showed that the combination of EFdA and TFV had an effect on the inhibition of HIV replication in cell culture (16). This was an unexpected finding as both NRTIs are analogs of dA. A partial explanation is provided in the present study where we show examples of template sites where TFV is not incorporated efficiently (Fig. 7*A*, *lane 3*, faint band at template position +6), whereas EFdA-MP very efficiently blocked RT with both ICT and DCT mechanisms (Fig. 7*A*, *lane 2*, strong bands at template positions +6 and +7). Differences in the mechanism of activation to their respective active forms may partially be responsible for the lack of competition between EFdA and TFV (16).

Although $T/P_{EFdA\text{-}MP}$ is generally ideally located to undergo phosphorolytic excision, with EFdA-MP positioned at the N-site (Fig. 8) (24, 30, 39), excision-based resistance is not a major pathway for resistance to EFdA (11).[5] This is likely because of the apparently high reincorporation efficiency of the newly excised EFdA-TP. Furthermore, as shown in Fig. 6, when EFdA-MP is incorporated as a DCT, $T/P_{EFdA\text{-}MP\text{-}dTMP}$ is protected from excision, resulting in decreased drug resistance by the excision mechanism. Moreover, we did not observe excision of EFdA-MP-terminated primers in positions where EFdA-MP is incorporated as a mismatch (Fig. 6*C*). These data are consistent with our earlier cell-based data demonstrating that EFdA maintains its potency against HIV strains that carry excision-based zidovudine resistance mutations (11).

There are two nucleos(t)ide analog drugs that retain a 3′-OH and have been approved for the treatment of viral infections: entecavir, which is the most potent anti-hepatitis B virus nucleoside analog drug (45, 46), and sofosbuvir, which is a recently approved anti-hepatitis C virus nucleotide analog drug (47, 48). So far, there are no NRTIs with a 3′-OH group that are approved for the treatment of HIV infections. EFdA could be paired with approved anti-HIV drugs, leading to synergistic and

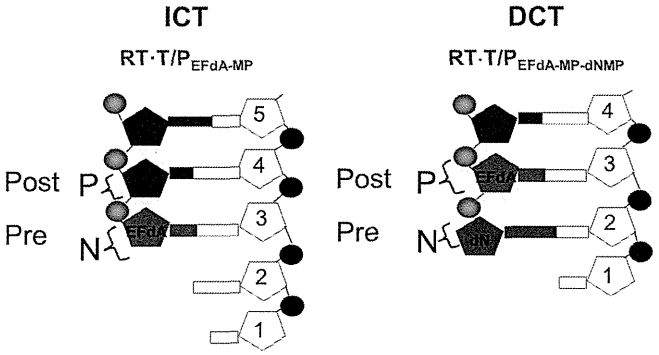

FIGURE 8. **Schematic representation of EFdA-MP-containing complexes.** EFdA acts as an ICT by occupying the N-site of RT, whereas it occupies the P-site of RT when it acts as a DCT. In this case, the N-site is free for the next incoming dNMP to be incorporated.

[5] B. Marchand, X. Tu, K. Kirby, E. Michailidis, O. Ihenacho, E. Kodama, H. Mitsuya, M. Parniak, and S. Sarafianos, unpublished data.

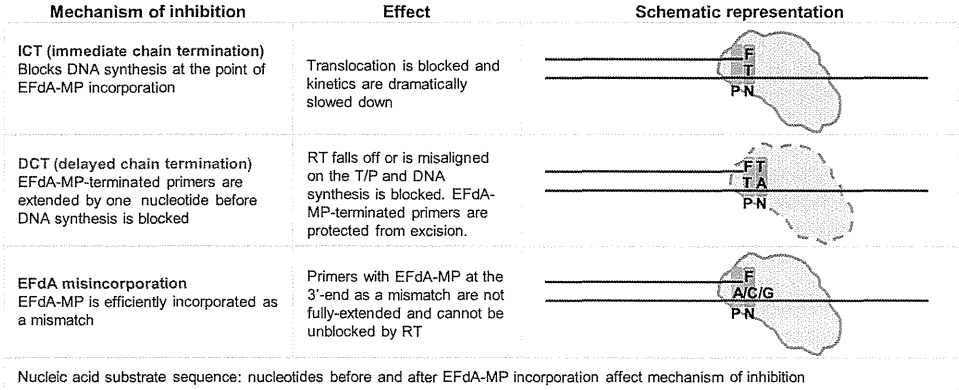

FIGURE 9. **Overview of the multiple mechanisms of RT inhibition by EFdA.**

additive effects as shown in cell-based assays, and it also suppressed viral loads in macaques to undetectable levels within a week of treatment and without any signs of toxicity (9, 11, 16, 17, 44). Its ability to inhibit RT by multiple mechanisms imparts excellent antiviral activity (11) and may contribute to its favorable resistance profile (49), thus rendering it a potentially promising new generation NRTI.

REFERENCES

1. Hammer, S. M., Saag, M. S., Schechter, M., Montaner, J. S., Schooley, R. T., Jacobsen, D. M., Thompson, M. A., Carpenter, C. C., Fischl, M. A., Gazzard, B. G., Gatell, J. M., Hirsch, M. S., Katzenstein, D. A., Richman, D. D., Vella, S., Yeni, P. G., and Volberding, P. A. (2006) Treatment for adult HIV infection: 2006 recommendations of the International AIDS Society–U.S.A. panel. *Top. HIV Med.* **14,** 827–843
2. Schinazi, R. F., Hernandez-Santiago, B. I., and Hurwitz, S. J. (2006) Pharmacology of current and promising nucleosides for the treatment of human immunodeficiency viruses. *Antiviral Res.* **71,** 322–334
3. Parniak, M. A., and Sluis-Cremer, N. (2000) Inhibitors of HIV-1 reverse transcriptase. *Adv. Pharmacol.* **49,** 67–109
4. De Clercq, E. (2007) Anti-HIV drugs. *Verh. K. Acad. Geneeskd. Belg.* **69,** 81–104
5. Sluis-Cremer, N., and Tachedjian, G. (2008) Mechanisms of inhibition of HIV replication by non-nucleoside reverse transcriptase inhibitors. *Virus Res.* **134,** 147–156
6. Deval, J. (2009) Antimicrobial strategies: inhibition of viral polymerases by 3′-hydroxyl nucleosides. *Drugs* **69,** 151–166
7. Sharma, P. L., Nurpeisov, V., Hernandez-Santiago, B., Beltran, T., and Schinazi, R. F. (2004) Nucleoside inhibitors of human immunodeficiency virus type 1 reverse transcriptase. *Curr. Top. Med. Chem.* **4,** 895–919
8. Sarafianos, S. G., Marchand, B., Das, K., Himmel, D. M., Parniak, M. A., Hughes, S. H., and Arnold, E. (2009) Structure and function of HIV-1 reverse transcriptase: molecular mechanisms of polymerization and inhibition. *J. Mol. Biol.* **385,** 693–713
9. Kodama, E. I., Kohgo, S., Kitano, K., Machida, H., Gatanaga, H., Shigeta, S., Matsuoka, M., Ohrui, H., and Mitsuya, H. (2001) 4′-Ethynyl nucleoside analogs: potent inhibitors of multidrug-resistant human immunodeficiency virus variants *in vitro*. *Antimicrob. Agents Chemother.* **45,** 1539–1546
10. Michailidis, E., Marchand, B., Kodama, E. N., Singh, K., Matsuoka, M., Kirby, K. A., Ryan, E. M., Sawani, A. M., Nagy, E., Ashida, N., Mitsuya, H., Parniak, M. A., and Sarafianos, S. G. (2009) Mechanism of inhibition of HIV-1 reverse transcriptase by 4′-ethynyl-2-fluoro-2′-deoxyadenosine triphosphate, a translocation-defective reverse transcriptase inhibitor. *J. Biol. Chem.* **284,** 35681–35691
11. Kawamoto, A., Kodama, E., Sarafianos, S. G., Sakagami, Y., Kohgo, S., Kitano, K., Ashida, N., Iwai, Y., Hayakawa, H., Nakata, H., Mitsuya, H., Arnold, E., and Matsuoka, M. (2008) 2′-Deoxy-4′-C-ethynyl-2-halo-adenosines active against drug-resistant human immunodeficiency virus type 1 variants. *Int. J. Biochem. Cell Biol.* **40,** 2410–2420
12. Ohrui, H. (2006) 2′-Deoxy-4′-C-ethynyl-2-fluoroadenosine, a nucleoside reverse transcriptase inhibitor, is highly potent against all human immunodeficiency viruses type 1 and has low toxicity. *Chem. Rec.* **6,** 133–143
13. Kageyama, M., Nagasawa, T., Yoshida, M., Ohrui, H., and Kuwahara, S. (2011) Enantioselective total synthesis of the potent anti-HIV nucleoside EFdA. *Org. Lett.* **13,** 5264–5266
14. Gallois-Montbrun, S., Schneider, B., Chen, Y., Giacomoni-Fernandes, V., Mulard, L., Morera, S., Janin, J., Deville-Bonne, D., and Veron, M. (2002) Improving nucleoside diphosphate kinase for antiviral nucleotide analogs activation. *J. Biol. Chem.* **277,** 39953–39959
15. Kirby, K. A., Michailidis, E., Fetterly, T. L., Steinbach, M. A., Singh, K., Marchand, B., Leslie, M. D., Hagedorn, A. N., Kodama, E. N., Marquez, V. E., Hughes, S. H., Mitsuya, H., Parniak, M. A., and Sarafianos, S. G. (2013) Effects of 4′- and 2-substitutions on the bioactivity of 4′-ethynyl-2-fluoro-2′-deoxyadenosine. *Antimicrob. Agents Chemother.* **57,** 6254–6264
16. Hachiya, A., Reeve, A. B., Marchand, B., Michailidis, E., Ong, Y. T., Kirby, K. A., Leslie, M. D., Oka, S., Kodama, E. N., Rohan, L. C., Mitsuya, H., Parniak, M. A., and Sarafianos, S. G. (2013) Evaluation of combinations of 4′-ethynyl-2-fluoro-2′-deoxyadenosine with clinically used antiretroviral drugs. *Antimicrob. Agents Chemother.* **57,** 4554–4558
17. Murphey-Corb, M., Rajakumar, P., Michael, H., Nyaundi, J., Didier, P. J., Reeve, A. B., Mitsuya, H., Sarafianos, S. G., and Parniak, M. A. (2012) Response of simian immunodeficiency virus to the novel nucleoside reverse transcriptase inhibitor 4′-ethynyl-2-fluoro-2′-deoxyadenosine *in vitro* and *in vivo*. *Antimicrob. Agents Chemother.* **56,** 4707–4712
18. Bauman, J. D., Das, K., Ho, W. C., Baweja, M., Himmel, D. M., Clark, A. D., Jr., Oren, D. A., Boyer, P. L., Hughes, S. H., Shatkin, A. J., and Arnold, E. (2008) Crystal engineering of HIV-1 reverse transcriptase for structure-based drug design. *Nucleic Acids Res.* **36,** 5083–5092
19. Schuckmann, M. M., Marchand, B., Hachiya, A., Kodama, E. N., Kirby, K. A., Singh, K., and Sarafianos, S. G. (2010) The N348I mutation at the connection subdomain of HIV-1 reverse transcriptase decreases binding to nevirapine. *J. Biol. Chem.* **285,** 38700–38709
20. Ndongwe, T. P., Adedeji, A. O., Michailidis, E., Ong, Y. T., Hachiya, A., Marchand, B., Ryan, E. M., Rai, D. K., Kirby, K. A., Whatley, A. S., Burke, D. H., Johnson, M., Ding, S., Zheng, Y. M., Liu, S. L., Kodama, E., Delviks-Frankenberry, K. A., Pathak, V. K., Mitsuya, H., Parniak, M. A., Singh, K., and Sarafianos, S. G. (2012) Biochemical, inhibition and inhibitor resistance studies of xenotropic murine leukemia virus-related virus reverse transcriptase. *Nucleic Acids Res.* **40,** 345–359
21. Kirby, K. A., Marchand, B., Ong, Y. T., Ndongwe, T. P., Hachiya, A., Michailidis, E., Leslie, M. D., Sietsema, D. V., Fetterly, T. L., Dorst, C. A., Singh, K., Wang, Z., Parniak, M. A., and Sarafianos, S. G. (2012) Structural and inhibition studies of the RNase H function of xenotropic murine leukemia virus-related virus reverse transcriptase. *Antimicrob. Agents Chemother.* **56,** 2048–2061
22. Michailidis, E., Ryan, E. M., Hachiya, A., Kirby, K. A., Marchand, B., Leslie, M. D., Huber, A. D., Ong, Y. T., Jackson, J. C., Singh, K., Kodama, E. N., Mitsuya, H., Parniak, M. A., and Sarafianos, S. G. (2013) Hypersusceptibility mechanism of tenofovir-resistant HIV to EFdA. *Retrovirology* **10,** 65
23. Michailidis, E., Singh, K., Ryan, E. M., Hachiya, A., Ong, Y. T., Kirby, K. A., Marchand, B., Kodama, E. N., Mitsuya, H., Parniak, M. A., and Sarafianos, S. G. (2012) Effect of translocation defective reverse transcriptase inhibitors on the activity of N348I, a connection subdomain drug resistant HIV-1 reverse transcriptase mutant. *Cell. Mol. Biol.* **58,** 187–195
24. Sarafianos, S. G., Clark, A. D., Jr., Tuske, S., Squire, C. J., Das, K., Sheng, D., Ilankumaran, P., Ramesha, A. R., Kroth, H., Sayer, J. M., Jerina, D. M., Boyer, P. L., Hughes, S. H., and Arnold, E. (2003) Trapping HIV-1 reverse transcriptase before and after translocation on DNA. *J. Biol. Chem.* **278,** 16280–16288
25. Meyer, P. R., Matsuura, S. E., So, A. G., and Scott, W. A. (1998) Unblocking of chain-terminated primer by HIV-1 reverse transcriptase through a nucleotide-dependent mechanism. *Proc. Natl. Acad. Sci. U.S.A.* **95,** 13471–13476
26. Singh, K., Marchand, B., Rai, D. K., Sharma, B., Michailidis, E., Ryan, E. M., Matzek, K. B., Leslie, M. D., Hagedorn, A. N., Li, Z., Norden, P. R., Hachiya, A., Parniak, M. A., Xu, H. T., Wainberg, M. A., and Sarafianos, S. G. (2012) Biochemical mechanism of HIV-1 resistance to rilpivirine. *J. Biol. Chem.* **45,** 38110–38123
27. Johnson, K. A. (1993) Conformational coupling in DNA polymerase fidelity. *Annu. Rev. Biochem.* **62,** 685–713
28. Sarafianos, S. G., Clark, A. D., Jr., Das, K., Tuske, S., Birktoft, J. J., Ilankumaran, P., Ramesha, A. R., Sayer, J. M., Jerina, D. M., Boyer, P. L., Hughes, S. H., and Arnold, E. (2002) Structures of HIV-1 reverse transcriptase with pre- and post-translocation AZTMP-terminated DNA. *EMBO J.* **21,** 6614–6624
29. Hachiya, A., Kodama, E. N., Schuckmann, M. M., Kirby, K. A., Michailidis, E., Sakagami, Y., Oka, S., Singh, K., and Sarafianos, S. G. (2011) K70Q adds high-level tenofovir resistance to "Q151M complex" HIV reverse transcriptase through the enhanced discrimination mechanism. *PLoS One* **6,** e16242
30. Marchand, B., and Gotte, M. (2003) Site-specific footprinting reveals differences in the translocation status of HIV-1 reverse transcriptase. Implications for polymerase translocation and drug resistance. *J. Biol. Chem.*

278, 35362–35372
31. Biaglow, J. E., and Kachur, A. V. (1997) The generation of hydroxyl radicals in the reaction of molecular oxygen with polyphosphate complexes of ferrous ion. *Radiat. Res.* **148,** 181–187
32. Hu, W. S., and Hughes, S. H. (2012) HIV-1 reverse transcription. *Cold Spring Harb. Perspect. Med.* **2,** a006882
33. Huang, H., Chopra, R., Verdine, G. L., and Harrison, S. C. (1998) Structure of a covalently trapped catalytic complex of HIV-1 reverse transcriptase: implications for drug resistance. *Science* **282,** 1669–1675
34. Tuske, S., Sarafianos, S. G., Clark, A. D., Jr., Ding, J., Naeger, L. K., White, K. L., Miller, M. D., Gibbs, C. S., Boyer, P. L., Clark, P., Wang, G., Gaffney, B. L., Jones, R. A., Jerina, D. M., Hughes, S. H., and Arnold, E. (2004) Structures of HIV-1 RT-DNA complexes before and after incorporation of the anti-AIDS drug tenofovir. *Nat. Struct. Mol. Biol.* **11,** 469–474
35. Das, K., Bandwar, R. P., White, K. L., Feng, J. Y., Sarafianos, S. G., Tuske, S., Tu, X., Clark, A. D., Jr., Boyer, P. L., Hou, X., Gaffney, B. L., Jones, R. A., Miller, M. D., Hughes, S. H., and Arnold, E. (2009) Structural basis for the role of the K65R mutation in HIV-1 reverse transcriptase polymerization, excision antagonism, and tenofovir resistance. *J. Biol. Chem.* **284,** 35092–35100
36. Lansdon, E. B., Samuel, D., Lagpacan, L., Brendza, K. M., White, K. L., Hung, M., Liu, X., Boojamra, C. G., Mackman, R. L., Cihlar, T., Ray, A. S., McGrath, M. E., and Swaminathan, S. (2010) Visualizing the molecular interactions of a nucleotide analog, GS-9148, with HIV-1 reverse transcriptase-DNA complex. *J. Mol. Biol.* **397,** 967–978
37. Muftuoglu, Y., Sohl, C. D., Mislak, A. C., Mitsuya, H., Sarafianos, S. G., and Anderson, K. S. (2014) Probing the molecular mechanism of action of the HIV-1 reverse transcriptase inhibitor 4′-ethynyl-2-fluoro-2′-deoxyadenosine (EFdA) using pre-steady-state kinetics. *Antiviral Res.* **106,** 1–4
38. Kim, J., Roberts, A., Yuan, H., Xiong, Y., and Anderson, K. S. (2012) Nucleocapsid protein annealing of a primer-template enhances (+)-strand DNA synthesis and fidelity by HIV-1 reverse transcriptase. *J. Mol. Biol.* **415,** 866–880
39. Arion, D., Kaushik, N., McCormick, S., Borkow, G., and Parniak, M. A. (1998) Phenotypic mechanism of HIV-1 resistance to 3′-azido-3′-deoxythymidine (AZT): increased polymerization processivity and enhanced sensitivity to pyrophosphate of the mutant viral reverse transcriptase. *Biochemistry* **37,** 15908–15917
40. Meyer, P. R., Matsuura, S. E., Mian, A. M., So, A. G., and Scott, W. A. (1999) A mechanism of AZT resistance: an increase in nucleotide-dependent primer unblocking by mutant HIV-1 reverse transcriptase. *Mol. Cell* **4,** 35–43
41. Sarafianos, S. G., Hughes, S. H., and Arnold, E. (2004) Designing anti-AIDS drugs targeting the major mechanism of HIV-1 RT resistance to nucleoside analog drugs. *Int. J. Biochem. Cell Biol.* **36,** 1706–1715
42. Boyer, P. L., Sarafianos, S. G., Arnold, E., and Hughes, S. H. (2001) Selective excision of AZTMP by drug-resistant human immunodeficiency virus reverse transcriptase. *J. Virol.* **75,** 4832–4842
43. Meyer, P. R., Smith, A. J., Matsuura, S. E., and Scott, W. A. (2004) Effects of primer-template sequence on ATP-dependent removal of chain-terminating nucleotide analogues by HIV-1 reverse transcriptase. *J. Biol. Chem.* **279,** 45389–45398
44. Vu, B. C., Boyer, P. L., Siddiqui, M. A., Marquez, V. E., and Hughes, S. H. (2011) 4′-C-Methyl-2′-deoxyadenosine and 4′-C-ethyl-2′-deoxyadenosine inhibit HIV-1 replication. *Antimicrob. Agents Chemother.* **55,** 2379–2389
45. Woo, G., Tomlinson, G., Nishikawa, Y., Kowgier, M., Sherman, M., Wong, D. K., Pham, B., Ungar, W. J., Einarson, T. R., Heathcote, E. J., and Krahn, M. (2010) Tenofovir and entecavir are the most effective antiviral agents for chronic hepatitis B: a systematic review and Bayesian meta-analyses. *Gastroenterology* **139,** 1218–1229
46. Michailidis, E., Kirby, K. A., Hachiya, A., Yoo, W., Hong, S. P., Kim, S. O., Folk, W. R., and Sarafianos, S. G. (2012) Antiviral therapies: focus on hepatitis B reverse transcriptase. *Int. J. Biochem. Cell Biol.* **44,** 1060–1071
47. Lawitz, E., Mangia, A., Wyles, D., Rodriguez-Torres, M., Hassanein, T., Gordon, S. C., Schultz, M., Davis, M. N., Kayali, Z., Reddy, K. R., Jacobson, I. M., Kowdley, K. V., Nyberg, L., Subramanian, G. M., Hyland, R. H., Arterburn, S., Jiang, D., McNally, J., Brainard, D., Symonds, W. T., McHutchison, J. G., Sheikh, A. M., Younossi, Z., and Gane, E. J. (2013) Sofosbuvir for previously untreated chronic hepatitis C infection. *N. Engl. J. Med.* **368,** 1878–1887
48. Gentile, I., Borgia, F., Buonomo, A. R., Castaldo, G., and Borgia, G. (2013) A novel promising therapeutic option against hepatitis C virus: an oral nucleotide NS5B polymerase inhibitor sofosbuvir. *Curr. Med. Chem.* **20,** 3733–3742
49. Maeda, K., Desai, D. V., Aoki, M., Nakata, H., Kodama, E. N., and Mitsuya, H. (2014) Delayed emergence of HIV-1 variants resistant to 4′-ethynyl-2-fluoro-2′-deoxyadenosine: comparative sequential passage study with lamivudine, tenofovir, emtricitabine and BMS-986001. *Antiviral Ther.* **19,** 179–189

Organic & Biomolecular Chemistry

PAPER

View Article Online
View Journal | View Issue

Cite this: Org. Biomol. Chem., 2014, 12, 6842

Design and synthesis of potent macrocyclic HIV-1 protease inhibitors involving P1–P2 ligands†

Arun K. Ghosh,*[a] Gary E. Schiltz,[a] Linah N. Rusere,[a] Heather L. Osswald,[a] D. Eric Walters,[b] Masayuki Amano[c] and Hiroaki Mitsuya[c,d]

Received 7th April 2014,
Accepted 27th June 2014

DOI: 10.1039/c4ob00738g

www.rsc.org/obc

A series of potent macrocyclic HIV-1 protease inhibitors have been designed and synthesized. The compounds incorporated 16- to 19-membered macrocyclic rings between a nelfinavir-like P2 ligand and a tyrosine side chain containing a hydroxyethylamine sulfonamide isostere. All cyclic inhibitors are more potent than their corresponding acyclic counterparts. Saturated derivatives showed slight reduction of potency compared to the respective unsaturated derivatives. Compound **8a** containing a 16-membered ring as the P1–P2 ligand showed the most potent enzyme inhibitory and antiviral activity.

Introduction

HIV-1 protease inhibitors are a critical component of antiretroviral therapy (ART) for the treatment of patients with HIV infection and AIDS.[1,2] The use of ART has reduced both the mortality and morbidity rates among HIV-infected patients. However, the emergence of drug resistance has raised serious concerns about the prospects of long-term treatment options.[3,4] In our continuing studies to combat drug resistance, our structure-based design strategies targeting the protein backbone have led to the discovery of a variety of novel HIV-1 protease inhibitors (PIs), including the FDA approved HIV-1 protease inhibitor darunavir with broad-spectrum activity against multidrug-resistant HIV-1 variants.[5–8]

In another approach to developing inhibitors with broad-spectrum activity, we have been exploring the design of various macrocyclic HIV-1 protease inhibitors. Recently, we have reported the design of a series of potent PIs that incorporate flexible macrocycles involving P1′–P2′-ligands and P1–P2 ligands to effectively fill in the S1′–S2′ and S1–S2 subsites of HIV-1 protease, respectively.[9–11] The concept of this macrocyclic design evolved from the observation that certain mutations lead to decreased van der Waals interactions and increased the size of the subsite hydrophobic pocket.[12,13] On the basis of this insight of enzyme flexibility in accommodating alternate packing, we designed flexible macrocycles between the P1′-side chain and a suitable P2′-ligand to fill in the S2′ and S1′-subsites. As shown in Fig. 1, this effort led to a series of potent macrocyclic inhibitors, as represented by inhibitor **2**, containing the P1–P2-ligands of darunavir.

In an alternate design approach, we have designed macrocyclic inhibitors as represented by inhibitor **3**, where the macrocycles involve the P1–P2 ligands, incorporating 2,3-dihydroxybenzoic acid derivatives as the P2-ligand, and aliphatic chains as the P1 ligand. Fairlie and co-workers also designed a number of different macrocyclic HIV-1 protease inhibitors, as represented in inhibitor **4**.[14] Based upon our previous results, we have now investigated macrocyclic inhibitors involving P1–P2 ligands which incorporate 3-hydroxy-2-alkylbenzoic acid derivatives as the P2-ligand and alkylated tyrosine side chains as the P1 ligand. In particular, as shown in Fig. 2, inhibitors are designed by taking advantage of the large hydrophobic pocket in the HIV-1 protease S1–S2 active site. These inhibitors incorporate the P2 ligand found in the FDA approved drug nelfinavir **5** and the P1′–P2′ ligands found in TMC-126 (**6**).[15,16] Various macrocyclic inhibitors can be synthesized conveniently by ring-closing metathesis of the dienes **7** using Grubbs' catalyst.

Results and discussion

In order to gain additional insight into the proposed inhibitors, a molecular model was obtained with one of the unsaturated macrocycles overlaid with nelfinavir (Fig. 3).[17] As can be seen, the phenolic hydroxyl group of the macrocyclic inhibitor

[a]*Departments of Chemistry and Medicinal Chemistry, Purdue University, West Lafayette, IN 47907, USA. E-mail: akghosh@purdue.edu; Fax: +1 765 4961612; Tel: +1 765 4945323*
[b]*Department of Pharmaceutical Sciences, Rosalind Franklin University of Medicine and Science, North Chicago, IL 60064, USA*
[c]*Kumamoto University School of Medicine, Department of Hematology and Infectious diseases, Kumamoto 860-8556, Japan*
[d]*Experimental Retrovirology Section, HIV and AIDS Malignancy Branch, National Cancer Institute, Bethesda, Maryland 20892, USA*

†Electronic supplementary information (ESI) available: Characterization of new compounds; copies of ^{1}H NMR and ^{13}C-NMR spectra are available. See DOI: 10.1039/c4ob00738g

This journal is © The Royal Society of Chemistry 2014

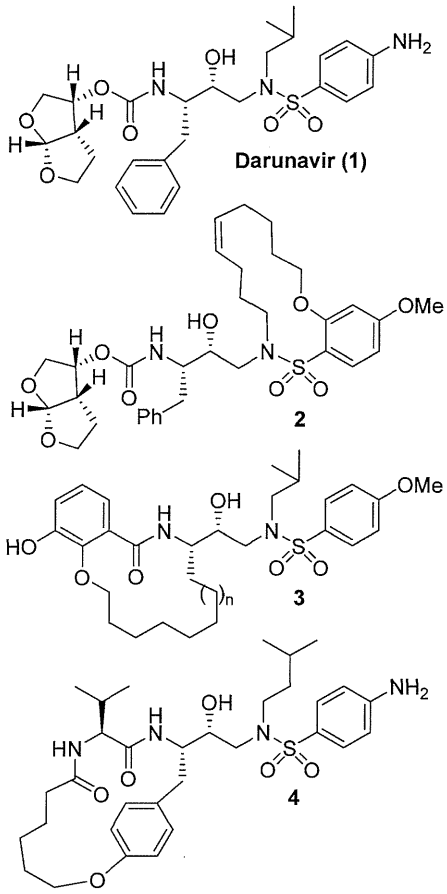

Fig. 1 Structures of Darunavir and macrocyclic HIV-1 protease inhibitors **2–4**.

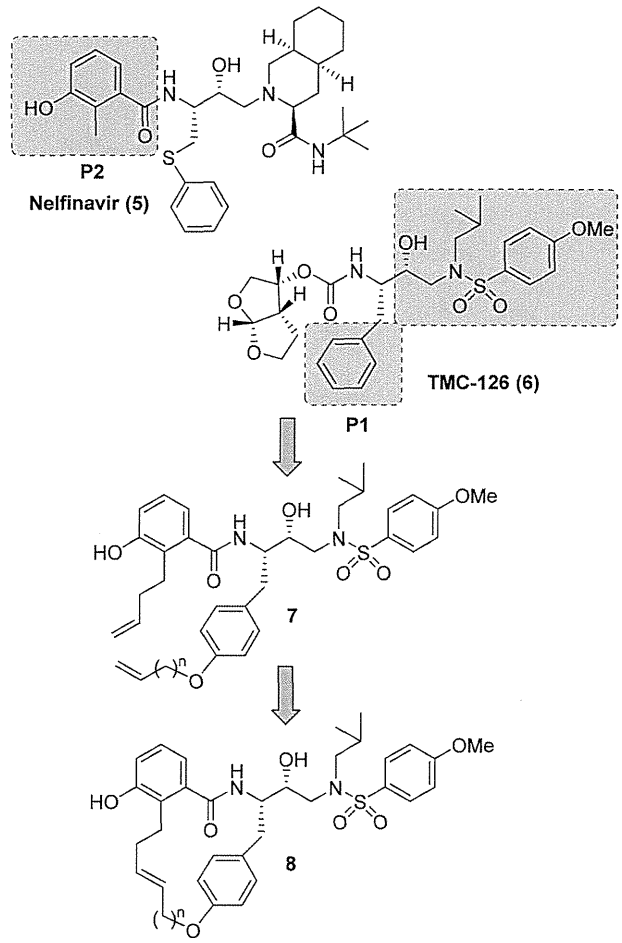

Fig. 2 Design of macrocyclic inhibitor **8**.

8a (16-membered macrocycle, $n = 1$) appears to be capable of forming hydrogen bonds with the Asp30 backbone NH as well as the side chain carbonyl residue in the S2 subsite. The benzamide carbonyl oxygen is positioned to form a hydrogen bond with the tight-bound water molecule that can interact with one of the sulfonamide oxygens. The 4-methoxy oxygen on the P2′-sulfonamide ligand can also form hydrogen bonding interactions with the Asp30′ backbone NH in the S2′-pocket. Furthermore, it appears that as the ring size increases, the P_2 and P_1 ligands would become distorted from their optimal position and bind less tightly in the S2 pockets. Based upon this model, it appears that inhibitors with 16–18 membered ring sizes could optimally fit in the S2 hydrophobic pocket.

Synthesis of the desired tyrosine-derived hydroxyethylamine sulfonamide isostere is shown in Scheme 1. The commercially available butadiene monoxide **9** was reacted with *p*-benzyloxyphenylmagnesium bromide in the presence of a catalytic amount of cuprous cyanide to provide the corresponding allylic alcohol.[18] Sharpless asymmetric epoxidation of the resulting alcohol using (−)-diethyl D-tartrate provided optically active epoxide **10** in very good yield.[19,20] Regioselective epoxide opening of **10** using $TMSN_3$ and $Ti(O\text{-}iPr)_4$ as described by Sharpless and co-workers afforded the corresponding azido diol.[21] The resulting diol was converted to epoxide **11** by treatment with 2-acetoxyisobutyryl chloride in chloroform followed by reaction of the resulting chloroacetate with sodium methoxide.[22]

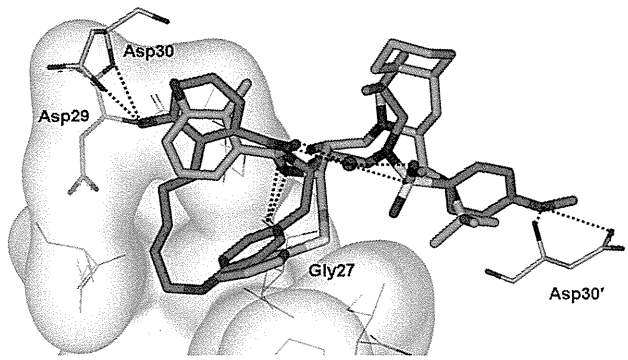

Fig. 3 Model of inhibitor **8a** (green, $n = 1$) overlaid with nelfinavir (magenta) in the HIV-1 protease active site.

Preparation of the elaborated sulfonamide intermediate was accomplished by opening epoxide **11** with isobutylamine in 2-propanol at reflux.[23] The resulting amine was reacted with *p*-methoxyphenylsulfonyl chloride in the presence of aqueous

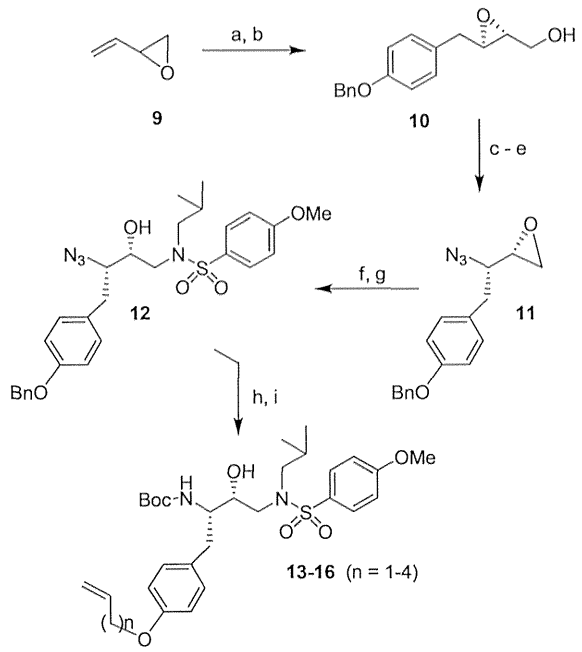

Scheme 1 Reagents and conditions: (a) *p*-BnOPhMgBr, CuCN, THF, –78 °C; 39%; (b) D(–)-DET, $Ti(O\text{-}iPr)_4$, 4 A MS, TBHP, CH_2Cl_2, 79%; (c) $Ti(O\text{-}iPr)_4$, $TMSN_3$, PhH, reflux, 55%; (d) $AcOMe_2CCOCl$, $CHCl_3$; (e) NaOMe, THF, 71%, over 2 steps; (f) *i*-$BuNH_2$, *i*-PrOH, reflux; (g) *p*-$MeOPhSO_2Cl$, aq. $NaHCO_3$, CH_2Cl_2, 97% 2 steps; (h) H_2, MeOH, Boc_2O, Pd/C, 75%; (i) acetone, K_2CO_3, alkenyl bromide, reflux, 94–96%.

$NaHCO_3$ to provide azidosulfonamide **12** in excellent yield. Catalytic hydrogenation of **12** over Pd/C in the presence of Boc_2O provided the Boc-protected amine as well as the free phenol in an efficient one-pot operation. The resulting phenol derivative was alkylated with an appropriate alkenylbromide in acetone in the presence of K_2CO_3 to furnish the requisite olefins **13–16** in excellent yields.

Synthesis of 3-hydroxy-2-alkenylbenzoic acid, the corresponding alkenyl metathesis substrate, is shown in Scheme 2.

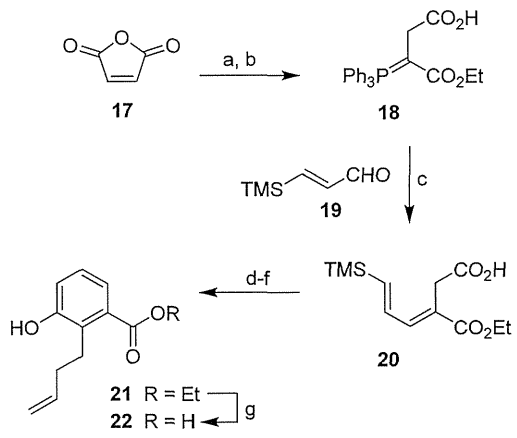

Scheme 2 Reagents and conditions: (a) PPh_3, acetone; (b) EtOH, 35%, over 2 steps; (c) $PhCH_3$, hydroquinone, 83%; (d) LDA, THF, DMPU, 4-bromo-1-butene; (e) TFAA, Et_3N; (f) $NaBH_4$, EtOH, 48%, over 2 steps; (g) KOH, MeOH, reflux, 89%.

Phosphorane **18** was prepared from maleic anhydride **17** using reported procedures.[24–26] Wittig reaction of phosphorane **18** with known[27,28] aldehyde **19** provided dienoic acid **20** in good yield (83%).[29] Alkylation of **20** with LDA and 4-bromo-1-butene in the presence of DMPU afforded the corresponding triene derivative. This was exposed to trifluoroacetic anhydride (TFAA) and triethylamine followed by $NaBH_4$ in ethanol which effected a 1,6-electrocyclization to afford benzoic acid ester **21**.[30] Saponification of ethyl ester **21** with KOH in methanol provided the desired acid **22**.

Synthesis of various acyclic and macrocyclic inhibitors is shown in Scheme 3. Treatment of Boc-derivatives **13–16** with trifluoroacetic acid in CH_2Cl_2 resulted in the deprotection of the Boc group. The resulting amines were then coupled with acid **22** to provide acyclic dienes **7a–d** in good yields. Ring-closing metathesis of the dienes **7a–d** was carried out using Grubbs' first generation catalyst in CH_2Cl_2 at 23 °C for 4 h to provide macrocycles **8a–d** in excellent yields (78–89%).[31,32] The alkenes were formed as a mixture of *trans*/*cis* isomers. *Trans*/*cis* Ratios of the unsaturated macrocycles were 1 : 1 for **8a** (16-membered ring); 3 : 1 for **8b** (17-membered ring); 5 : 1 for **8c** (18-membered ring); and essentially a single *trans*-isomer for **8d** (19-membered ring). The *cis*/*trans* isomers could not be separated by silica gel chromatography. To obtain the corresponding saturated macrocyclic inhibitors, we first attempted hydrogenation of allyl ether **8a** over 10% Pd/C in ethyl acetate for 12 h. However, under these conditions, only the ring

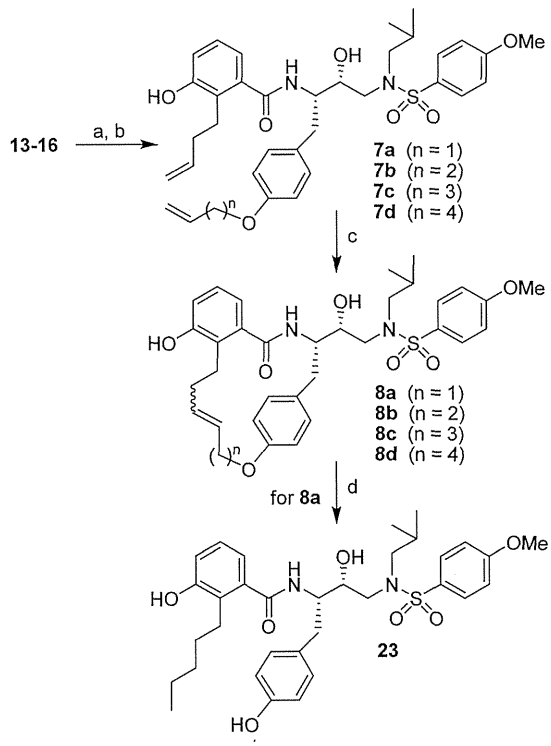

Scheme 3 Reagents and conditions: (a) TFA, CH_2Cl_2; (b) acid **22**, EDCI, HOBt, Et_3N, DMF, 60–78%, over 2 steps; (c) Grubbs' 1st Gen. Cat. (20 mol%), CH_2Cl_2, 23 °C, 78–89%; (d) H_2, Pd/C, EtOAc.

This journal is © The Royal Society of Chemistry 2014

opened compound **23** was isolated as the main product. The use of PtO_2 as a catalyst also resulted in an allylic ring cleavage to afford the ring-opened product. A similar effect had been reported by us in the context of the synthesis of cycloamide based HIV-1 protease inhibitors.[11]

To prevent cleavage of the allylic ether, we carried out the hydrogenation according to the procedure reported by Sajiki and Hirota.[33] As shown in Scheme 4, hydrogenation of **8a** in the presence of 5% Pd/C in 1% NH_3 in methanol for 4 hours afforded the saturated macrocyclic inhibitor **24a** in 40% isolated yield. This condition also provided the ring opened compound **23** as the byproduct (27%). Catalytic hydrogenation of unsaturated macrocycles **8b–8d** however, proceeded smoothly over 10% Pd/C in ethyl acetate to provide saturated derivatives **24b–d** respectively in excellent yields (88–94%).

The inhibitory potencies of acyclic and cyclic inhibitors were measured by the assay protocol of Toth and Marshall.[34] The results are shown in Tables 1 and 2. A number of selected compounds that showed potent enzyme inhibitory K_i values were further evaluated in an antiviral assay. Antiviral activity was determined based on a previously published assay protocol.[35] As can be seen, acyclic inhibitors in Table 1 displayed enzyme inhibitory potency ranging from 5 nM to 45 nM. An acyclic ring opened product with a P1-tyrosine side chain (compound **23**) showed enhanced potency (K_i = 0.41 nM). In general, inhibitors with a longer chain showed reduction in potency. Interestingly, conversion of acyclic inhibitors to their corresponding cyclic derivatives after RCM resulted in significant improvement in enzyme inhibitory activity. As shown in Table 2, acyclic inhibitor **7a** (K_i = 5 nM and antiviral IC_{50} > 1μM) upon RCM provided 16-membered macrocycles **8a** (E/Z = 1 : 1) which showed a K_i value of 0.2 nM. The mixture of isomers also displayed an antiviral IC_{50} value of 0.21 μM in MT-2 cells. Saturation of double bonds provided a saturated inhibitor **24a** which showed a comparable enzyme inhibitory activity. An acyclic inhibitor **7b** (K_i = 7 nM) following RCM afforded a cyclic inhibitor **8b** (E/Z = 3 : 1) which also showed improvement of enzyme K_i over its acyclic derivatives. The 17-membered macrocycles showed a comparable antiviral activity to 16-membered inhibitors. The corresponding saturated inhibitor **24b** displayed reduction in inhibitory potency (K_i = 2.3 nM). However, this compound maintained a similar antiviral activity as its unsaturated mixtures.

An acyclic inhibitor **7c** upon cyclization provided a cyclic inhibitor **8c** (E/Z = 5 : 1) which displayed K_i of 10 nM and an antiviral activity of 420 nM. Interestingly, the corresponding saturated derivative **24c** showed improvement in enzyme inhibitory activity. The antiviral activity of inhibitor **24c** was reduced nearly by a factor of 2 over its unsaturated derivative. An acyclic inhibitor **7d** (K_i = 30 nM) was subjected to RCM and provided a cyclic derivative **8d** as a single *E*-isomer. This compound showed improvement in enzyme K_i over its acyclic derivative. Saturation of the double bond in **8d** provided a saturated derivative **24d** which showed 5-fold reduction in inhibitory activity.

To gain insight into specific ligand-binding site interactions, an energy minimized model structure of inhibitor **24b** was created. The structure was modelled in the HIV-1 protease active site based on our published X-ray crystal structure of inhibitor **1** and HIV-1 protease complex (Protein Data Bank entry 1S6G) as a template.[36] As can be seen in Fig. 4, the 3-hydroxy group of the P2-ligand appeared to be within proximity to form a hydrogen bond with Asp30 backbone NH as well as with the side chain carboxylic acid. The P2-carbonyl group appears to form effective hydrogen bonds with the tight-bound structural water molecule through one of the P2′-sulfonamide oxygens. The macrocyclic carbon chain is nicely accommodated in the S1–S2 hydrophobic pockets. Interestingly, saturation of the ring olefin in **8b** resulted in a more flexible carbon chain which may have resulted in unfavorable van der Waals interactions in the S2-subsite. This may explain the reduction of enzyme inhibitory activity for compound **24b**. It appears that the 16-membered saturated macrocycle in **24a** makes more favorable interactions in the S2-subsite of the protease active site than the corresponding 17-membered macrocycle in compound **24b**. The OMe-group on the P2′-sulfonamide of inhibitor **24b** appears to maintain hydrogen bonding interactions with Asp30′ backbone NH as well as with the side chain carboxylic acid.

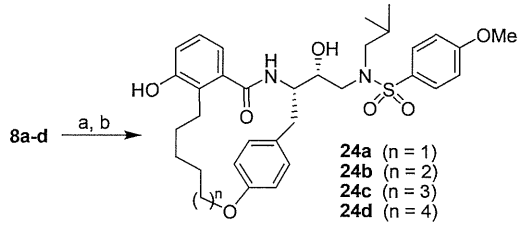

Scheme 4 Reagents and conditions: (a) for n = 1, H_2, 5% Pd/C, 1% NH_3 in MeOH, 40%; (b) for n = 2–4, H_2, Pd/C, EtOAc, 88–94%.

Table 1 Potency (K_i) of acyclic inhibitors

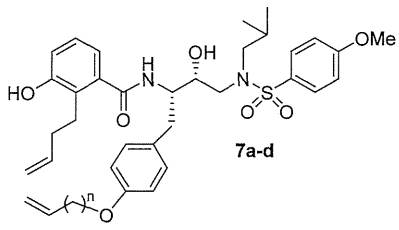

Compd	Ring size (after RCM)	n	K_i [a] (nM)
7a	16	1	5
7b	17	2	7
7c	18	3	45
7d	19	4	30
23	—	—	0.41

[a] Darunavir exhibited K_i = 16 pM.

Table 2 Enzymatic inhibitory and antiviral activity of macrocyclic inhibitors

Entry	Inhibitor	K_i (nM)	IC_{50} [a,b] (μM)	Entry	Inhibitor	K_i (nM)	IC_{50} [a,b] (μM)
1	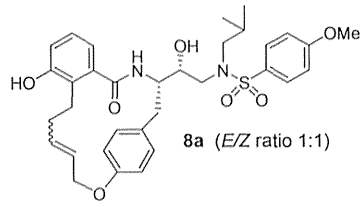 **8a** (*E*/*Z* ratio 1:1)	0.2	0.21	5	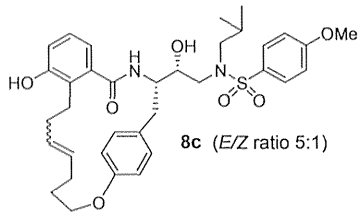 **8c** (*E*/*Z* ratio 5:1)	10	0.42
2	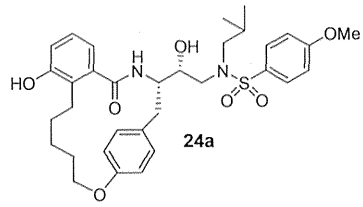 **24a**	0.25	nt	6	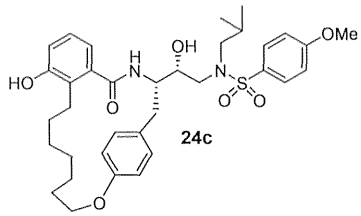 **24c**	4	0.80
3	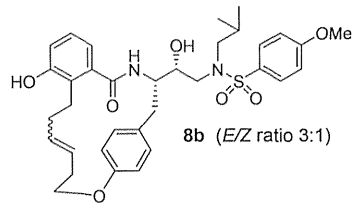 **8b** (*E*/*Z* ratio 3:1)	0.5	0.28	7	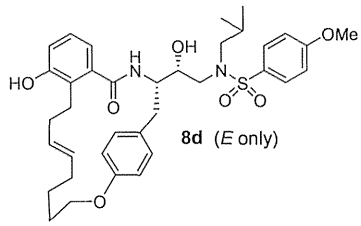 **8d** (*E* only)	4	nt
4	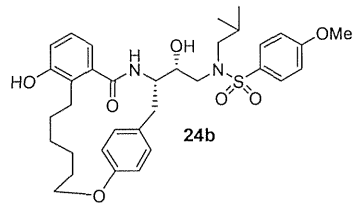 **24b**	2.3	0.31	8	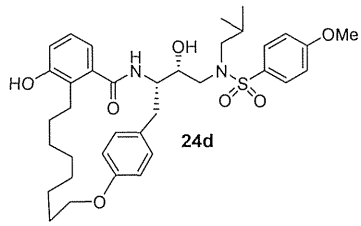 **24d**	20	nt

[a] Human T-lymphoid (MT-2) cells were exposed to 100 $TCID_{50}$ values of HIV-1LAI and cultured in the presence of each PI, and IC_{50} values were determined using the MTT assay. Darunavir exhibited K_i = 16 pM, IC_{50} = 0.003 μM. [b] nt = not tested.

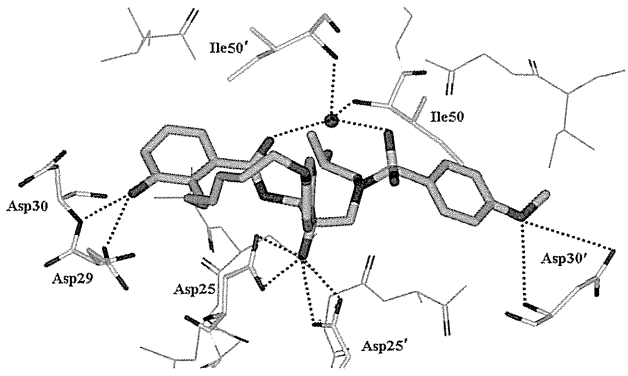

Fig. 4 An energy-minimized model of 17-membered macrocyclic inhibitor **24b** in the HIV-1 protease active site. Putative hydrogen bonds are shown as dotted lines.

Conclusions

In summary, a novel series of macrocyclic HIV-1 protease inhibitors has been designed, synthesized and evaluated. The design of macrocycles is based on the hypothesis that the cyclic flexible chain would effectively pack the hydrophobic pocket in the S1 to S2 subsites. We have synthesized acyclic derivatives involving P1-tyrosine and P2-3-hydroxy-2-alkenylbenzamide derivatives. Ring-closing metathesis using Grubbs' 1st generation catalyst efficiently provided 16–19 membered macrocyclic rings containing both *E*/*Z* olefins as the P1–P2 ligands in these inhibitors. Catalytic hydrogenation provided the corresponding saturated derivatives. In general, all cyclic inhibitors containing *E*/*Z* olefins showed improved enzyme inhibitory potency compared to their acyclic counterparts. The saturated derivatives are less potent than the corresponding unsaturated derivatives. Compound **8a** showed the best enzyme inhibitory and antiviral activity in this series. A model of the *E*-isomer of **8b** was created to obtain ligand-binding site interactions. As it appears, the unsaturated macrocyclic ring is nicely accommodated in the S1–S2 hydrophobic pocket. Saturation of the ring olefin most likely resulted in unfavorable van der Waals interaction in the S2-subsite. This may explain the reduction of enzyme inhibitory activity for the saturated compound **24b**.

This journal is © The Royal Society of Chemistry 2014

One of the important features of these macrocyclic inhibitors is that the inhibitors contain only two asymmetric centers and can be synthesized efficiently using RCM reaction. Further design and optimization of these inhibitors are in progress.

Experimental section

All reactions were carried out under an inert atmosphere, either N_2 or Ar, using magnetic stirring and oven-dried glassware. All solvents were anhydrous and distilled prior to use. Dichloromethane and triethylamine were distilled from calcium hydride. Tetrahydrofuran, diethyl ether, and benzene were distilled from sodium/benzophenone. All other solvents were of HPLC grade or better. Flash column chromatography was performed using EM Science 60–200 mesh silica gel. Thin-layer chromatography was performed using 60 F-254 E. Merck silica gel plates. ^{1}H- and ^{13}C-NMR were recorded using Bruker AV-500, Avance DRX-500, Varian Mercury-Vx-300, and Gemini-2300 spectrometers and Me_4Si as an internal standard. Infrared spectra were recorded on an ATI Mattson Genesis Series FT-IR. Optical rotations were recorded on a Perkin-Elmer 341 polarimeter. A Thermo Finnigan LCQ Classic mass spec was used for MS analyses.

(2*R*,3*R*)-3-(4-benzyloxybenzyl-oxiran-2yl)-methanol (10)

To a suspension of magnesium turnings (101.6 mg, 4.2 mmol) in 25 mL THF was added a solution of 4-benzyloxybromobenzene (1.0 g, 3.8 mmol) in THF. The mixture was heated at 65 °C for 30 min and the solution was cooled to room temperature. Grignard solution was added dropwise to a solution of CuCN (26 mg, 0.30 mmol) and butadiene monoxide **9** (220 mg, 3.1 mmol) in 80 mL of anhydrous THF at −78 °C. The reaction was stirred for 30 min at −78 °C, after which it was quenched with 15 mL of saturated NH_4Cl followed by 15 mL of NH_4OH. The aqueous layer was extracted twice with ethyl acetate. The combined organic phases were dried over sodium sulfate and concentrated *in vacuo*. The residue was purified by flash chromatography on silica gel with 15–20% ethyl acetate–hexanes to give *trans*-4-(4-benzyloxy)phenyl-2-buten-1-ol (308 mg, 1.21 mmol, 39% yield). ^{1}H-NMR (500 MHz, $CDCl_3$) δ 7.44 (d, 2H, J = 7.0 Hz), 7.39 (dt, 2H, J = 2.0, 7.0 Hz), 7.33 (tt, 1H, J = 2.5, 7.5 Hz), 7.11 (td, 2H, J = 2.5, 9.0 Hz), 6.92 (td, 2H, J = 2.0, 8.5 Hz), 5.84 (dtt, 1H, J = 1.5, 6.5, 15.0 Hz), 5.69 (dtt, 1H, J = 1.5, 6.0, 15.5 Hz), 5.05 (s, 2H), 4.12 (dd, 2H, J = 1.0, 55 Hz), 3.34 (d, 2H, J = 7.0 Hz), 1.48 (s, 1H); ^{13}C-NMR (125 MHz, $CDCl_3$) δ 157.3, 137.2, 132.4, 132.0, 130.0, 129.6, 128.6, 128.0, 127.5, 114.9, 70.1, 63.6, 37.8.

Molecular sieves (500 mg) were flame dried in a flask and then allowed to cool to room temperature. Dry dichloromethane (4 mL) and D-DET (11 mg, 0.05 mmol) were added and the suspension was cooled to −25 °C. To this, Ti(O*i*-Pr)$_4$ (20.7 μL, 0.07 mmol) and TBHP (0.35 mL, 1.92 mmol) were added and the mixture was stirred at −25 °C for 30 minutes. A solution of *trans*-4-(4-benzyloxy)phenyl-2-buten-1-ol (211 mg, 0.87 mmol) in dry DCM (1 mL) was added to the above mixture and it was kept in a freezer at about −25 °C for 18 h. To the reaction mixture H_2O (3 mL) was added and stirred at 0 °C for 30 minutes. A 10% aqueous NaOH solution was then added and the mixture was warmed to room temperature for 1 h. The product was extracted with DCM (3×), dried with Na_2SO_4, filtered, and concentrated under reduced pressure. Purification by flash column chromatography (30–40% EtOAc–hexanes) afforded epoxy alcohol **10** (177 mg, 79%). $[\alpha]_D^{23}$ +12.5° (*c* 0.14 $CHCl_3$); ^{1}H-NMR (500 MHz, $CDCl_3$) δ 7.45 (d, 2H, J = 7.0 Hz), 7.41, (t, 2H, J = 5.5 Hz), 7.34 (t, 1H, J = 7.5 Hz), 7.17 (td, 2H, J = 2.0, 8.5 Hz), 6.95 (td, 2H, J = 2.0, 8.5 Hz), 5.06 (s, 2H), 3.88 (dd, 1H, J = 2.5, 12.5 Hz), 3.60 (dd, 1H, J = 4.5, 12.5 Hz), 3.17 (dt, 1H, J = 2.5, 5.5 Hz), 2.98 (m, 1H), 2.86 (m, 2H); ^{13}C-NMR (125 MHz, $CDCl_3$) δ 157.7, 137.1, 130.1, 129.3, 128.6, 128.0, 127.5, 115.0, 70.1, 61.6, 58.4, 56.2, 37.0.

(1*S*,2*R*)-2-[1-Azido-2-(4-benzyloxyphenyl)-ethyl]-oxirane (11)

Dry benzene (5 mL), Ti(O*i*-Pr)$_4$ (160 μL), and $TMSN_3$ (72 μL) were refluxed for 5 hours. A solution of epoxy alcohol **10** (0.123 g, 0.455 mmol) in dry benzene (3 mL) was added and the solution was refluxed for 30 minutes. After cooling to room temperature, 5% H_2SO_4 (2 mL) was added and the solution was stirred at room temperature for 1 hour. The layers were separated and the aqueous portion was extracted with ethyl acetate (3×). The organic solution was dried with Na_2SO_4, filtered, and concentrated under reduced pressure. Purification by flash column chromatography (40–50% EtOAc–hexanes) gave (2*R*,3*S*)-3-azido-4-(4-benzyloxyphenyl)-1,2-butanediol (78.9 mg, 55% yield). $[\alpha]_D^{23}$ +18.1° (*c* 0.19 $CHCl_3$); ^{1}H-NMR (500 MHz, $CDCl_3$) δ 7.44 (d, 2H, J = 7.0 Hz), 7.39 (t, 2H, J = 7.5 Hz), 7.34 (t, 1H, J = 7.0 Hz), 7.19 (d, 2H, J = 8.5 Hz), 6.95 (td, 2H, J = 2.0, 8.5 Hz), 5.05 (s, 2H), 3.80–3.67 (m, 4H), 3.26 (bs, 1H), 2.99 (dd, 1H, J = 3.0, 14.0 Hz), 2.77–2.73 (m, 2H); ^{13}C-NMR (125 MHz, $CDCl_3$) δ 157.8, 137.0, 130.4, 129.5, 128.6, 128.0, 127.6, 115.1, 73.1, 70.1, 65.7, 63.3, 36.2; HRMS *m*/*z* $(M + Na)^+$ calcd for $C_{17}H_{19}N_3O_3Na$ 336.1324, found 336.1317.

(2*R*,3*S*)-3-Azido-4-(4-benzyloxyphenyl)-1,2-butanediol (84.4 mg, 0.269 mmol) and chloroform (3 mL) were cooled to 0 °C. 1-Chlorocarbonyl-1-methylethyl acetate (58.5 μL, 0.404 mmol) was added and the solution was stirred at room temperature for 20 hours. A saturated solution of $NaHCO_{3(aq)}$ was added and the mixture stirred for 15 minutes. The crude chloroacetate was extracted with chloroform, dried with Na_2SO_4, filtered, and concentrated *in vacuo*. The residue was dissolved in dry THF (5 mL) and cooled to 0 °C. Solid NaOMe (24.7 mg) was added and the reaction mixture was stirred at room temperature for 2 hours. The reaction was quenched with saturated $NH_4Cl_{(aq)}$ and extracted with ethyl acetate. Drying over Na_2SO_4, filtering, and concentrating under reduced pressure afforded a residue which was purified by flash column chromatography (12% EtOAc–hexanes) to afford pure azido epoxide **11** (56.5 mg, 71% yield). $[\alpha]_D^{23}$ +11.3° (*c* 0.34 $CHCl_3$); ^{1}H-NMR (500 MHz, $CDCl_3$) δ 7.44 (d, 2H, J = 7.5 Hz), 7.40 (t, 2H, J = 8.0 Hz), 7.34 (t, 1H, J = 7.0 Hz), 7.17 (d, 2H, J = 11.0 Hz), 6.95 (td, 2H, J = 2.0, 11.5 Hz), 5.06 (s, 2H), 3.56 (quintet, 1H, J = 4.0, 5.0 Hz), 3.07–3.05

(m, 1H), 2.94 (dd, 1H, J = 4.5, 14.0 Hz), 2.84–2.82 (m, 1H), 2.81–2.75 (m, 2H); ^{13}C-NMR (125 MHz, $CDCl_3$) δ 157.9, 137.0, 130.4, 128.9, 128.6, 128.0, 127.5, 115.0, 70.1, 63.8, 53.0, 45.2, 37.4.

(2*R*,3*S*)-*N*-[3-Azido-4-(4-benzyloxyphenyl)-2-hydroxy-butyl]-*N*-isobutyl-4-methoxy-benzenesulfonamide (12)

To epoxide **11** (0.60 g, 2.03 mmol) in isopropanol (10 mL), was added isobutylamine (2 mL) and the solution was refluxed for 2 hours. The reaction was concentrated *in vacuo* and used as it is in the next reaction. The residue was taken up in DCM (10 mL), saturated aqueous $NaHCO_3$ (2 mL) and 4-methoxy-benzenesulfonyl chloride (0.50 g) were added and the reaction was stirred for 18 hours at room temperature. The organic layer was separated and the aqueous portion was extracted with DCM. The combined organics were dried with Na_2SO_4, filtered, and concentrated under reduced pressure. Flash column chromatography (15–25% EtOAc–hexanes) afforded sulfonamide **12** (1.06 g, 97% yield over 2 steps). ^{1}H-NMR (500 MHz, $CDCl_3$) δ 7.75 (dd, 2H, J = 2.0, 9.0 Hz), 7.45–7.43 (m, 2H), 7.39 (t, 2H, J = 7.5 Hz), 7.34–7.33 (m, 1H), 7.19 (d, 2H, J = 9.0 Hz), 7.01 (dd, 2H, J = 2.0, 9.0 Hz), 6.94 (dd, 2H, J = 2.0, 8.5 Hz), 5.06 (s, 2H), 3.83 (s, 3H), 3.78–3.75 (m, 1H), 3.59–3.55 (m, 2H), 3.24 (dd, 1H, J = 9.5, 15.5 Hz), 3.09–3.02 (m, 3H), 2.80 (dd, 1H, J = 6.5, 13.5 Hz), 2.75 (dd, 1H, J = 9.0, 14.0 Hz), 1.71–1.69 (m, 1H), 0.94 (d, 3H, J = 6.5 Hz), 0.88 (d, 3H, J = 6.5 Hz); ^{13}C-NMR (125 MHz, $CDCl_3$) δ 163.2, 157.8, 137.0, 130.4, 129.7, 129.5, 128.6, 128.0, 127.5, 115.1, 114.5, 71.8, 70.0, 66.7, 58.9, 55.7, 52.9, 36.0, 27.2, 20.2, 19.8; HRMS *m/z* $(M + Na)^+$ calcd for $C_{28}H_{34}N_4O_5SNa$ 561.2148, found 561.2166.

(1*S*,2*R*)-{1-(4-Allyloxy-benzyl)-2-hydroxy-3-[isobutyl-(4-methoxy-benzenesulfonyl)-amino]-propyl}-carbamic acid *tert*-butyl ester (13)

Azide **12** (55.1 mg, 0.10 mmol) was dissolved in methanol (5 mL) and Boc_2O (27 mg) and 10% Pd/C (10 mg) were added and the reaction mixture was stirred under an H_2 atmosphere for 18 hours. The mixture was filtered through Celite and concentrated under reduced pressure. Flash column chromatography (30% EtOAc–hexanes) afforded (1*S*,2*R*)-{2-hydroxy-1-(4-hydroxybenzyl)-3-[isobutyl-(4-methoxy-benzenesulfonyl)-amino]-propyl}-carbamic acid *tert*-butyl ester (40 mg, 75% yield). ^{1}H-NMR (500 MHz, $CDCl_3$) δ 7.68 (d, 2H, J = 8.5 Hz), 7.06 (m, 2H), 6.96 (d, 2H, J = 9.0 Hz), 6.73–6.71 (m, 2H), 6.35–6.25 (bs, 1H), 4.78 (d, 1H, J = 8.0 Hz), 4.01–3.99 (m, 1H), 3.84 (s, 3H), 3.81–3.79 (m, 1H), 3.71–3.69 (m, 1H), 3.10–2.77 (m, 6H), 1.86–1.81 (m, 1H), 0.89–0.85 (m, 6H); ^{13}C-NMR (125 MHz, $CDCl_3$) δ 163.0, 156.3, 154.7, 130.6, 129.8, 129.5, 129.3, 115.4, 114.4, 80.0, 72.8, 58.6, 55.6, 54.9, 53.6, 34.6, 28.3, 27.2, 20.1, 19.9.

The above phenol derivative (13 mg, 0.02 mmol) was dissolved in acetone (2 mL), K_2CO_3 (5.2 mg) and allyl bromide (22 μL) were added, and the reaction was refluxed for 16 hours, and then concentrated under reduced pressure. Flash column chromatography (25% EtOAc–hexanes) afforded allylic ether **13** (13.4 mg, 96% yield). ^{1}H-NMR (500 MHz, $CDCl_3$) δ 7.69 (dd, 2H, J = 2.0, 6.5 Hz), 7.15 (d, 2H, J = 8.5 Hz), 6.97 (dd, 2H, J = 2.0, 7.0 Hz), 6.85 (dd, 2H, J = 2.0, 6.5 Hz), 6.08–6.02 (m, 1H), 5.41 (dd, 1H, J = 1.5, 17.5 Hz), 5.28 (dd, 1H, J = 1.0, 10.5 Hz), 4.62–4.61 (m, 1H), 4.51 (dt, 2H, J = 1.5, 5.5 Hz), 3.86 (s, 3H), 1.35 (s, 9H), 0.90 (d, 3H, J = 6.5 Hz), 0.86 (d, 3H, J = 6.5 Hz); ^{13}C-NMR (125 MHz, $CDCl_3$) δ 163.0, 157.3, 156.1, 133.4, 130.5, 129.9, 129.5, 117.6, 114.8, 114.6, 114.3, 79.7, 72.7, 68.8, 58.7, 55.6, 54.7, 53.8, 34.5, 28.3, 27.2, 20.2, 19.9.

(1*S*,2*R*)-{1-(4-(3-Butenyloxy)-benzyl)-2-hydroxy-3-[isobutyl-(4-methoxy-benzenesulfonyl)-amino]-propyl}-carbamic acid *tert*-butyl ester (14)

(1*S*,2*R*)-{2-Hydroxy-1-(4-hydroxybenzyl)-3-[isobutyl-(4-methoxy-benzenesulfonyl)-amino]-propyl}-carbamic acid *tert*-butyl ester (36.4 mg, 0.07 mmol) was dissolved in acetone (5 mL). To this was added K_2CO_3 (24 mg) and 4-bromo-1-butene (7 μL) and the reaction was refluxed for 18 hours. After concentrating under reduced pressure, the product was purified by flash column chromatography (25% EtOAc–hexanes) to afford **14** (37 mg, 96% yield). ^{1}H-NMR (500 MHz, $CDCl_3$) δ 7.69 (dd, 2H, J = 2.0, 9.0 Hz), 7.14 (d, 2H, J = 8.5 Hz), 6.96 (dd, 2H, J = 2.0, 9.0 Hz), 6.83 (d, 2H, J = 9.0 Hz), 5.94–5.86 (m, 1H), 5.16 (ddd, 1H, J = 1.5, 2.0, 17.0 Hz), 5.10 (ddd, 1H, J = 1.0, 1.5, 10.0 Hz), 4.64 (d, 1H, J = 8.0 Hz), 3.98 (t, 2H, J = 7.0 Hz), 3.94–3.92 (m, 1H), 3.86 (s, 3H), 3.78–3.75 (m, 1H), 3.71–3.68 (m, 1H), 3.10–2.77 (m, 6H), 2.55–2.51 (m, 2H), 1.84–1.79 (m, 1H), 1.35 (s, 9H), 0.89 (d, 3H, J = 6.5 Hz), 0.85 (d, 3H, J = 6.5 Hz); ^{13}C-NMR (125 MHz, $CDCl_3$) δ 163.0, 157.6, 156.1, 134.5, 130.5, 130.0, 129.8, 129.5, 117.0, 114.6, 114.3, 79.6, 72.7, 67.2, 58.6, 55.6, 54.7, 53.8, 34.5, 29.3, 28.3, 27.2, 20.2, 19.9.

(1*S*,2*R*)-2-Hydroxy-3-[isobutyl-(4-methoxy-benzenesulfonyl)-amino]-1-(4-(4-pentenyloxy)-benzyl)-propyl]-carbamic acid *tert*-butyl ester (15)

(1*S*,2*R*)-{2-Hydroxy-1-(4-hydroxybenzyl)-3-[isobutyl-(4-methoxy-benzenesulfonyl)-amino]-propyl}-carbamic acid *tert*-butyl ester (54.8 mg, 0.105 mmol), K_2CO_3 (43.5 mg), and 5-bromo-1-pentene (62 μL) were added to acetone (3 mL). The mixture was refluxed for 18 hours, and then concentrated under reduced pressure. Flash column chromatography (30% EtOAc–hexanes) afforded olefin **15** (59.6 mg, 94% yield). ^{1}H-NMR (500 MHz, $CDCl_3$) δ 7.69 (d, 2H, J = 8.0 Hz), 7.14 (d, 2H, J = 8.5 Hz), 6.96 (dd, 2H, J = 2.0, 7.0 Hz), 6.82 (d, 2H, J = 8.5 Hz), 5.89–5.80 (m, 1H), 5.05 (ddd, 1H, J = 1.5, 2.0, 17.0 Hz), 4.99 (dd, 1H, J = 1.5, 10.0 Hz), 4.65 (d, 1H, J = 8.0 Hz), 3.94 (t, 2H, J = 6.5 Hz), 3.86 (s, 3H), 3.77 (m, 1H), 3.70 (m, 1H), 3.07–3.03 (m, 2H), 2.95–2.86 (m, 3H), 2.81–2.77 (m, 1H), 2.23 (q, 2H, J = 7.0 Hz), 1.90–1.82 (m, 3H), 1.35 (s, 9H), 0.90–0.86 (m, 6H); ^{13}C-NMR (125 MHz, $CDCl_3$) δ 163.0, 157.7, 156.1, 137.9, 130.5, 130.0, 129.6, 129.5, 115.2, 114.5, 114.3, 79.6, 72.7, 67.2, 58.6, 55.6, 54.7, 53.7, 34.5, 30.1, 28.5, 28.3, 27.2, 20.2, 19.9; HRMS *m/z* $(M + Na)^+$ calcd for $C_{31}H_{46}N_2O_7SNa$ 613.2923, found 613.2906.

This journal is © The Royal Society of Chemistry 2014

(1*S*,2*R*)-{1-(4-(5-Hexenyloxy)-benzyl)-2-hydroxy-3-[isobutyl-(4-methoxy-benzenesulfonyl)-amino]-propyl}-carbamic acid *tert*-butyl ester (16)

(1*S*,2*R*)-{2-Hydroxy-1-(4-hydroxybenzyl)-3-[isobutyl-(4-methoxy-benzenesulfonyl)-amino]-propyl}-carbamic acid *tert*-butyl ester (51.5 mg, 0.0985 mmol), K_2CO_3 (41 mg), and 6-bromo-1-hexene (66 μL) were added to acetone (3 mL). The mixture was refluxed for 16 hours, and then concentrated under reduced pressure. Flash column chromatography (25% EtOAc–hexanes) afforded olefin **16** (58.5 mg, 96% yield). ^{1}H-NMR (500 MHz, $CDCl_3$) δ 7.69 (ddt, 2H, J = 3.0, 8.5 Hz), 7.14 (d, 2H, J = 8.5 Hz), 6.96 (ddt, 2H, J = 2.5, 9.0 Hz), 6.82 (d, 2H, J = 8.5 Hz), 5.86–5.78 (m, 1H), 5.04 (ddd, 1H, J = 1.5, 2.0, 17.0 Hz), 4.96 (ddd, 1H, J = 1.0, 2.0, 10.5 Hz), 4.65 (d, 1H, J = 8.5 Hz), 3.93 (t, 2H, J = 6.5 Hz), 3.86 (s, 3H), 3.77 (m, 1H), 3.70 (m, 1H), 3.07–3.02 (m, 2H), 2.93–2.86 (m, 3H), 2.81–2.78 (m, 1H), 2.12 (q, 2H, J = 7.0 Hz), 1.85–1.76 (m, 3H), 1.59–1.53 (m, 2H), 1.35 (s, 9H), 0.89 (d, 3H, J = 6.5 Hz), 0.86 (d, 3H, J = 6.5 Hz); ^{13}C-NMR (125 MHz, $CDCl_3$) δ 163.0, 157.8, 156.1, 138.6, 130.5, 130.0, 129.6, 129.5, 114.8, 114.5, 114.3, 79.6, 72.7, 67.8, 58.6, 55.6, 54.7, 53.7, 34.5, 33.5, 28.8, 28.3, 27.2, 25.3, 20.2, 19.9; HRMS m/z $(M + Na)^+$ calcd for $C_{32}H_{48}N_2O_7S$ 627.3080, found 627.3087.

2-(Triphenylphosphoranylidene)-succinic acid 1-ethyl ester (18)

To a solution of acetone (100 mL) and PPh_3 (28.8 g, 0.11 mol) was added a solution of maleic anhydride (**17**, 10.8 g, 0.11 mol) in acetone (100 mL). After stirring at room temperature for 1 hour, the suspension was cooled to 0 °C. The product was isolated by filtering through a sintered glass funnel and washing with cold acetone. The product was then dried under vacuum. To the resulting solid, EtOH (200 mL) was added and the solution was stirred for 2 days after which the mixture was concentrated under reduced pressure. The carboxylic acid was recrystallized from 1 : 1 EtOAc–hexanes to afford **18** (15.8 g, 35% over 2 steps) as a tan solid. ^{1}H-NMR (500 MHz, $CDCl_3$) δ 7.63–7.59 (m, 9H), 7.51–7.47 (m, 6H), 3.80 (q, 2H, J = 7.0 Hz), 2.83 (d, 2H, J = 14.5 Hz), 0.75 (t, 3H, J = 7.0 Hz); ^{13}C-NMR (125 MHz, $CDCl_3$) δ 172.8, 172.7, 170.3, 133.8, 133.7, 133.7, 129.5, 129.4, 122.6, 121.8, 61.1, 39.6, 39.0, 35.2, 13.8.

3-Trimethylsilanyl-propenal (19)

Magnesium turnings (24.35 g, 1.00 mol) were added to dry THF (500 mL). Ethyl bromide (75 mL, 1.00 mmol) was slowly added dropwise by an addition funnel over 1.5 hours. The mixture was heated at 50 °C for 1 hour, and then cooled to 0 °C. Propargyl alcohol (20.8 mL, 0.36 mol) in dry THF (21 mL) was then added over 1 hour, and the mixture was stirred at room temperature overnight. The mixture was cooled to 0 °C and TMSCl (127 mL, 1.91 mol) was slowly added, followed by refluxing for 2 hours. After cooling to room temperature, 1.4 M H_2SO_4 (400 mL) was slowly added and the reaction was stirred for 10 minutes. The reaction was extracted with diethyl ether, washed with water, brine, dried with Na_2SO_4, and concentrated under reduced pressure. Short-path distillation afforded 3-trimethylsilanyl-1-hydroxy-2-propyne (39.9 g, 87% yield). ^{1}H-NMR (500 MHz, $CDCl_3$) δ 4.27 (s, 2H), 1.61 (s, 1H), 0.18 (s, 9H); ^{13}C-NMR (125 MHz, $CDCl_3$) δ 130.8, 90.8, 51.7, −0.2.

Dry diethyl ether (10 mL) and red-Al (6.2 mL, 21.8 mmol, 3.5 M in toluene) were cooled to 0 °C. 3-Trimethylsilanyl-1-hydroxy-2-propyne (1.86 g, 14.5 mmol) in dry ether (15 mL) was added dropwise and the solution was stirred at room temperature for 2 hours. The reaction was cooled to 0 °C and 3.6 M H_2SO_4 (15 mL) was added. After extraction with diethyl ether (3×), drying with Na_2SO_4, filtering, and concentrating under reduced pressure, the residue was purified by flash column chromatography (2–15% EtOAc–hexanes) to give 3-trimethylsilanyl-1-hydroxy-2-propene (1.19 g, 63% yield).

To 3-trimethylsilanyl-1-hydroxy-2-propene (0.11 g, 0.84 mmol) and dry DCM (5 mL) was added MnO_2 (0.51 g, 5.87 mmol) and the reaction mixture was stirred for 30 minutes at room temperature and 3 hours at reflux. After cooling to room temperature, 2 additional equivalents of MnO_2 were added and the mixture was stirred at room temperature for 16 hours. Silica gel was added, and the mixture was filtered through a silica gel plug after washing with DCM, and concentrated under reduced pressure to provide conjugated aldehyde **19** (102 mg, 95%). ^{1}H-NMR (300 MHz, $CDCl_3$) δ 9.49 (d, 1H J = 7.5 Hz), 7.19 (d, 1H, J = 18.9 Hz), 6.50 (dd, 1H, J = 7.5, 20.7 Hz), 0.17 (s, 9H); ^{13}C-NMR (75 MHz, $CDCl_3$) δ 194.7, 158.7, 144.0, −2.0.

(3*E*,5*E*)-3-Ethoxycarbonyl-6-trimethylsilyl-hexadienoic acid (20)

To a solution of aldehyde **19** (1.2 g, 7.8 mmol) in toluene (50 mL) was added Wittig reagent **18** (3.8 g, 9.4 mmol) and hydroquinone (8.6 mg) and the reaction was stirred for 2 days at room temperature. After concentrating the reaction mixture under reduced pressure, flash column chromatography (0–20% EtOAc–hexanes) afforded diene **20** (1.98 g, 83% yield). FT-IR (film) 1711, 1628, 1414, 1373, 1285, 1249, 1206, 1076, 990, 858, 841 cm^{-1}; ^{1}H-NMR (500 MHz, $CDCl_3$) δ 7.30 (d, 1H, J = 11.0 Hz), 6.72 (ddd, 1H, J = 1.0, 10.0, 18.0 Hz), 6.45 (d, 1H, J = 18.0 Hz), 4.23 (q, 2H, 7.0 Hz), 3.52 (s, 2H), 1.29 (dt, 3H, J = 1.0, 7.0 Hz), 0.12 (d, 9H, 1.0 Hz); ^{13}C-NMR (125 MHz, $CDCl_3$) δ 176.8, 167.5, 147.2, 143.0, 137.3, 123.5, 61.2, 32.5, 14.2, −1.6.

Ethyl-2-(3-butenyl)-3-hydroxybenzoate (21)

Diisopropylamine (2.41 mL, 17.19 mmol) and dry THF (50 mL) were cooled to 0 °C. To this, *n*-BuLi (11.5 mL, 18.4 mmol, 1.6 M in hexane) was added and the solution was stirred for 30 minutes at 0 °C. After adding DMPU (3.86 mL), acid **20** (2.05 g) in dry THF (10 mL) was added and the reaction mixture was stirred at 0 °C for 1 hour. After cooling the mixture to −78 °C, 4-bromo-1-butene (0.89 mL, 8.8 mmol) was added and the reaction mixture was stirred for 1 hour, followed by 2 hours at 0 °C. The reaction was quenched with 5% $HCl_{(aq)}$, extracted with diethyl ether, dried with Na_2SO_4, filtered, and concentrated under reduced pressure. Filtration through a 10 g silica gel column eluting with 15% EtOAc–

hexanes (100 mL) afforded the crude tris-olefin, which was used as is in the next step. Dry THF (10 mL) was added to the crude olefin (0.42 g, 1.35 mmol), followed by TFAA (0.38 mL) and TEA (0.57 mL). The reaction mixture was stirred at room temperature for 2 hours. The reaction was quenched with 5% $HCl_{(aq)}$ and extracted with diethyl ether. After drying with Na_2SO_4, filtration, and concentrating under reduced pressure, the residue was taken up in absolute ethanol (10 mL). The reaction was cooled to 0 °C and $NaBH_4$ (0.11 g, 2.71 mmol) was added. The mixture was stirred at room temperature for 2 hours, after which it was quenched with 5% $HCl_{(aq)}$. The crude product was extracted with diethyl ether, dried with Na_2SO_4, filtered, and concentrated *in vacuo*. Flash column chromatography (10% EtOAc–hexanes) afforded aromatic ester **21** (0.85 g, 48% yield, 2 steps). ^{1}H-NMR (500 MHz, $CDCl_3$) δ 7.40 (d, 1H, J = 1.0, 8.0 Hz), 7.11 (t, 1H, J = 8.0 Hz), 6.93 (dd, 1H, J = 1.0, 8.0 Hz), 5.98–5.90 (m, 1H), 5.31 (bs, 1H), 5.09 (ddd, 1H, J = 1.5, 3.5, 17.5 Hz), 4.99 (dd, 1H, J = 1.0, 10.0 Hz), 4.36 (q, 2H, J = 7.5 Hz), 3.01 (dd, 2H, J = 7.5, 9.5 Hz), 2.39–2.35 (m, 2H), 1.39 (t, 3H, J = 7.0 Hz); ^{13}C-NMR (125 MHz, $CDCl_3$) δ 168.2, 154.2, 138.5, 132.2, 129.2, 126.6, 122.7, 118.7, 115.0, 61.1, 34.0, 26.5, 14.3.

2-(3-Butenyl)-3-hydroxybenzoic acid (22)

Ester **21** (23.7 mg, 0.11 mmol) was taken up in MeOH (3 mL) and 2 N $KOH_{(aq)}$ (3 mL) was added. The reaction was refluxed for 36 hours. The MeOH was removed under reduced pressure and the aqueous mixture was acidified to pH = 2 with 6 N $HCl_{(aq)}$. Crude acid was extracted with EtOAc, dried with Na_2SO_4, filtered, and concentrated under reduced pressure. Flash column chromatography (20–50% EtOAc–hexanes) afforded pure acid **22** (18.5 mg, 89% yield). ^{1}H-NMR (500 MHz, $CDCl_3$) δ 7.61 (d, 1H, J = 8.0 Hz), 7.17 (t, 1H, J = 8.0 Hz), 7.01 (d, 1H, J = 8.0 Hz), 5.96 (m, 1H), 5.09 (dd, 1H, J = 1.5, 17.0 Hz), 5.01 (dd, 1H, J = 1.0, 10.0 Hz), 3.12 (t, 2H, J = 7.5 Hz), 2.39 (dd, 2H, J = 7.5, 15.5 Hz); ^{13}C-NMR (125 MHz, $CDCl_3$) δ 173.1, 154.2, 138.5, 130.6, 130.2, 126.7, 124.0, 119.9, 115.2, 34.0, 26.4. HRMS m/z $(M - H)^+$ calcd for $C_{11}H_{12}O_3$ 191.0708, found 191.0706.

(1*S*,2*R*)-*N*-{1-(4-Allyloxy-benzyl)-2-hydroxy-3-[isobutyl-(4-methoxy-benzenesulfonyl)-amino]-propyl}-2-(3-butenyl)-3-hydroxy-benzamide (7a)

Boc-amine **13** (8.1 mg, 0.014 mmol) was dissolved in DCM (1 mL) and stirred with 30% TFA–DCM (2 mL) for 2 hours at room temperature. After concentration under reduced pressure, the residue was taken up in DMF (2 mL). To the solution HOBt (2.1 mg), EDCI (3 mg), acid **22** (3 mg), and TEA (3 μL) were added. The reaction was stirred for 18 hours, and then brine was added. The crude product was extracted with ethyl acetate, dried with Na_2SO_4, filtered, and concentrated. Flash column chromatography (30–40% EtOAc–hexanes) afforded diene **7a** (6.4 mg, 70% yield over 2 steps). ^{1}H-NMR (500 MHz, $CDCl_3$) δ 7.68 (dd, 2H, J = 2.0, 7.0 Hz), 7.19 (d, 2H, J = 9.0 Hz), 6.98–6.95 (m, 2H), 6.92 (d, 1H, J = 8.0 Hz), 6.85 (d, 2H, J = 8.5 Hz), 6.75 (d, 1H, J = 8.0 Hz), 6.54 (d, 1H, J = 7.5 Hz), 6.28 (bs, 1H), 6.10–6.08 (m, 2H), 5.74–5.72 (m, 1H), 5.40 (dd, 1H, J = 1.5, 17.0 Hz), 5.28 (dd, 1H, J = 1.5, 10.5 Hz), 4.93 (dd, 1H, J = 1.5, 17.0 Hz), 4.88 (d, 1H, J = 10.0 Hz), 4.50 (d, 2H), 450–4.49 (m, 2H), 4.13–4.11 (m, 1H), 3.86 (s, 3H), 3.15–3.13 (m, 1H), 3.09–3.04 (m, 2H), 2.96–2.92 (m, 2H), 2.84–2.82 (m, 1H), 2.55–2.49 (m, 2H), 2.19–2.18 (m, 2H), 2.05–2.03 (m, 1H), 0.92 (d, 3H, J = 6.5 Hz), 0.87 (d, 3H, J = 6.5 Hz); ^{13}C-NMR (125 MHz, $CDCl_3$) δ 170.6, 163.1, 157.4, 154.5, 138.4, 137.6, 133.3, 130.3, 129.8, 129.7, 129.4, 126.9, 126.4, 118.7, 117.7, 117.1, 114.9, 114.9, 114.4, 73.1, 68.8, 58.9, 55.7, 54.3, 53.6, 33.9, 27.4, 26.5, 20.2, 19.9.

(1*S*,2*R*)-2-(3-Butenyl)-*N*-{1-(4-(3-butenyloxy)-benzyl)-2-hydroxy-3-[isobutyl-(4-methoxy-benzenesulfonyl)-amino]-propyl}-3-hydroxy-benzamide (7b)

Boc-protected amine **14** (0.15 g) and 30% TFA–DCM (2 mL) were stirred at room temperature for 2 hours, and then concentrated under vacuum. The residue was taken up in DMF (2 mL) and acid **22** (48.8 mg), EDCI (53.5 mg), HOBt (37.7 mg), and TEA (53 μL) were added. The solution was stirred at room temperature for 16 hours. Brine was added and the reaction mixture was extracted with EtOAc, dried over Na_2SO_4, filtered, and concentrated under reduced pressure. Flash column chromatography (30–50% EtOAc–hexanes) afforded diene **7b** (0.1295 g, 78% yield over 2 steps). ^{1}H-NMR (500 MHz, $CDCl_3$) δ 7.66 (d, 2H, J = 9.0 Hz), 7.17 (d, 2H, J = 8.5 Hz), 6.94 (d, 2H, J = 9.0 Hz), 6.88 (t, 1H, J = 7.5 Hz), 6.82 (d, 2H, J = 8.5 Hz), 6.75 (d, 1H, 7.5 Hz), 6.50 (d, 1H, J = 7.5 Hz), 6.19 (d, 1H, J = 8.5 Hz), 5.93–5.84 (m, 1H), 5.75–5.67 (m, 1H), 5.15 (ddd, 1H, J = 1.5, 2.0, 15.5 Hz), 5.09 (dd, 1H, J = 1.5 Hz, 10.5), 4.89 (dd, 1H, J = 1.5, 17.5 Hz), 4.83 (d, 1H, J = 10.0 Hz), 4.33–4.28 (m, 1H), 3.99–3.95 (m, 3H), 3.83 (s, 3H), 3.18–3.04 (m, 3H), 2.98–2.85 (m, 3H), 2.61–2.46 (m, 4H), 2.17 (q, 2H, J = 7.0, 7.5 Hz), 1.91–1.83 (m, 1H), 0.90 (d, 3H, J = 6.5 Hz), 0.86 (d, 3H, J = 6.5 Hz); ^{13}C-NMR (125 MHz, $CDCl_3$) δ 170.9, 163.1, 162.9, 157.7, 155.0, 138.6, 137.4, 134.5, 130.3, 129.7, 129.7, 129.4, 126.8, 126.5, 118.2, 117.1, 114.8, 114.6, 114.4, 73.0, 67.2, 58.8, 55.7, 54.3, 53.6, 33.9, 33.7, 31.7, 27.3, 26.5, 20.2, 19.9; HRMS m/z $(M + H)^+$ calcd for $C_{36}H_{47}N_2O_7S$ 651.3104, found 651.3098.

(1*S*,2*R*)-2-(3-Butenyl)-3-hydroxy-*N*-[2-hydroxy-3-[isobutyl-(4-methoxy-benzenesulfonyl)-amino]-1-(4-(4-pentenyloxy)-benzyl)-propyl]-benzamide (7c)

Boc-amine **15** (40.4 mg, 0.0668 mmol) and 30% TFA–DCM (4 mL) were stirred for 3 hours at room temperature, then concentrated *in vacuo*. The residue was taken up in DMF (2 mL) and acid **22** (12.8 mg), HOBt (9.0 mg), EDCI (12.8 mg), and TEA were stirred for 18 hours at room temperature. Brine was added and the product was extracted with ethyl acetate. After drying with Na_2SO_4, filtering, and concentrating under reduced pressure, the product was purified by flash column chromatography (30% EtOAc–hexanes) to afford diene **7c** (26.6 mg, 60% over 2 steps). ^{1}H-NMR (500 MHz, $CDCl_3$) δ 7.69 (d, 2H, J = 8.0 Hz), 7.19 (d, 2H, J = 8.5 Hz), 6.98–6.95 (m, 3H), 6.83 (d, 2H, J = 8.5 Hz), 6.77 (dd, 1H, J = 1.0, 8.0 Hz), 6.57 (dd, 1H, J = 1.0, 7.5 Hz), 6.02 (d, 1H, 8.5 Hz), 5.89–5.80 (m, 1H),

This journal is © The Royal Society of Chemistry 2014

5.78–5.72 (m, 1H), 5.65 (bs, 1H), 5.06 (ddd, 1H, J = 1.5, 2.0, 17.0 Hz), 5.00 (dd, 1H, J = 1.5, 10.0 Hz), 4.95 (dd, 1H, J = 1.5, 17.0 Hz), 4.90 (d, 1H), 4.33–4.29 (m, 1H), 4.24 (bs, 1H), 3.99–3.96 (m, 1H), 3.94 (t, 2H, J = 6.5 Hz), 3.87 (s, 3H), 3.15 (d, 1H, J = 8.5 Hz), 3.10–3.04 (m, 2H), 2.99–2.90 (m, 2H), 2.85–2.81 (m, 1H), 2.62–2.51 (m, 2H), 2.26–2.20 (m, 4H), 1.91–1.85 (m, 3H), 1.68–1.61 (m, 1H), 0.93 (d, 3H, J = 6.5 Hz), 0.88 (d, 3H, J = 6.5 Hz); ^{13}C-NMR (125 MHz, $CDCl_3$) δ 170.5, 163.1, 157.9, 154.3, 138.4, 137.8, 137.7, 130.3, 129.8, 129.4, 127.0, 126.3, 118.9, 117.1, 115.2, 115.0, 114.7, 114.4, 73.0, 67.2, 59.0, 55.7, 54.3, 53.7, 34.0, 30.1, 28.5, 27.4, 26.5, 20.2, 19.9; HRMS m/z $(M + Na)^+$ calc'd for $C_{37}H_{48}N_2O_7SNa$ 687.3080, found 637.3086.

(1*S*,2*R*)-2-(3-Butenyl)-*N*-{1-(4-(5-hexenyloxy)-benzyl)-2-hydroxy-3-[isobutyl-(4-methoxy-benzenesulfonyl)-amino]-propyl}-3-hydroxy-benzamide (7d)

Boc-amine **16** (37.8 mg, 0.061 mmol) and 30% TFA–DCM (5 mL) were stirred at room temperature for 6 hours, and then concentrated under reduced pressure. The residue was taken up in DMF (2 mL) and acid **22** (11.7 mg), EDCI (11.7 mg), HOBt (8.3 mg), and TEA (12.8 μL) were added and the reaction mixture was stirred at room temperature for 18 hours. Brine was added to the solution, and the product was extracted with ethyl acetate. After drying with Na_2SO_4, filtering, and concentrating under reduced pressure, the product was purified by flash column chromatography (25% EtOAc–hexanes) to afford diene **7d** (25.7 mg, 62% yield for 2 steps). ^{1}H-NMR (500 MHz, $CDCl_3$) δ 7.69 (d, 2H, J = 9.0 Hz), 7.19 (d, 2H, J = 8.5 Hz), 6.99–6.95 (m, 3H), 6.83 (d, 2H, J = 8.5 Hz), 6.77 (dd, 1H, J = 1.0, 8.0 Hz), 5.77 (dd, 1H, J = 1.0, 7.5 Hz), 6.04 (d, 1H, J = 9.0 Hz), 5.87–5.71 (m, 3H), 5.05 (ddd, 1H, J = 1.5, 2.0, 17.0 Hz), 4.98–4.93 (m, 2H), 4.99 (d, 1H, J = 10.0 Hz), 4.33–4.29 (m, 1H), 4.26–4.25 (bs, 1H), 3.99–3.96 (m, 1H), 3.93 (t, 2H, J = 6.5 Hz), 3.86 (s, 3H), 3.19–3.13 (m, 1H), 3.09–3.03 (m, 2H), 3.00–2.90 (m, 2H), 2.84–2.80 (m, 1H), 2.63–2.49 (m, 2H), 2.22–2.18 (m, 2H), 2.12 (q, 2H, J = 7.0 Hz), 1.91–1.85 (m, 1H), 1.82–1.76 (m, 2H), 1.60–1.53 (m, 2H), 0.93 (d, 3H, J = 6.5 Hz), 0.88 (d, 3H, J = 6.5 Hz); ^{13}C-NMR (125 MHz, $CDCl_3$) δ 170.5, 1631, 157.9, 154.3, 138.5, 138.4, 137.7, 130.3, 129.8, 129.4, 127.0, 126.4, 118.9, 117.1, 115.0, 114.9, 114.8, 114.7, 114.4, 73.0, 67.8, 59.0, 55.7, 54.3, 53.7, 34.0, 33.5, 29.7, 28.8, 27.4, 26.5, 25.4, 20.2, 19.9; HRMS m/z $(M + Na)^+$ calc'd for $C_{38}H_{50}N_2O_7SNa$ 701.3236, found 701.3217.

(2′*R*,3″*S*)-*N*-[2′-Hydroxy-2-(10-hydroxy-5-oxo-17-oxa-4-aza-tricyclo[16.2.2.06,11]docosa-1(21),6,8,10,14,18(22),19-heptaen-3″-yl)-ethyl]-*N*-isobutyl-4-methoxy-benzenesulfonamide (8a)

Diene **7a** (12 mg, 0.02 mmol) was dissolved in dry DCM (5 mL). Grubbs' first generation catalyst (2 mg) was added and the reaction mixture was stirred for 4 h. The solution was concentrated and purified by flash column chromatography (35% EtOAc–hexanes) to afford olefin **8a** (9.6 mg, 83% yield) as an inseparable 1 : 1 mixture of *cis*/*trans* isomers and a mixture of diastereomers. ^{1}H-NMR (500 MHz, $CDCl_3$) δ 7.76–7.73 (m, 4H), 7.02–6.87 (m, 12 H) 6.76–6.69 (m, 4 H), 5.86 (dd, 2H, J = 9.5, 21.5 Hz), 5.56–5.54 (m, 2H), 5.41–5.36 (m, 2H), 5.30–5.25 (m, 2H), 4.55–4.51 (m, 2H), 4.44–4.35 (m, 4H), 3.97–3.95 (m, 2H), 2.91–2.85 (m, 2H), 2.69–2.57 (m, 4H), 1.94–1.90 (m, 2H), 0.98 (dd, 3H, J = 2.5, 6.5 Hz), 0.92 (d, 3H, J = 6.5 Hz); ^{13}C-NMR (125 MHz, $CDCl_3$) δ 170.0, 169.7, 163.2, 157. 2, 155.8, 154.6, 139.8, 138.8, 137.5, 137.1, 133.0, 131.8, 131.2, 130.4, 129.6, 129.5, 128.7, 127.1, 126.9, 126.8, 125.2, 124.8, 124.3, 122.8, 122.3, 122.2, 122.1, 119.2, 118.9, 117.2, 116.5, 114.5, 73.8, 72.1, 70.0, 59.2, 55.7, 54.2, 54.0, 53.8, 34.8, 30.3, 29.7, 29.3, 27.4, 27.4, 26.6, 25.1, 20.2, 19.9; HRMS m/z $(M - H)^+$ calcd $C_{33}H_{39}N_2O_7S$ 607.2478, found 607.2479.

(2′*R*,3″*S*)-*N*-[2′-Hydroxy-2-(10-hydroxy-5-oxo-18-oxa-4-aza-tricyclo[17.2.2.06,11]tricosa-1(22),6,8,10,14,19(23),20-heptaen-3″-yl)-ethyl]-*N*-isobutyl-4-methoxy-benzene sulfonamide (8b)

Diene **7b** (7.5 mg) was dissolved in dry DCM (3 mL) and Grubbs' first generation catalyst (0.9 mg) was added. The reaction was stirred for 4 hours at room temperature, and then concentrated. Flash column chromatography (30–50% EtOAc–hexanes) gave olefin **8b** (5.6 mg, 78% yield) as an inseparable 3 : 1 (by ^{1}H-NMR analysis) mixture of isomers. ^{1}H-NMR (500 MHz, $CDCl_3$) δ 7.73 (d, 2H, J = 9.0 Hz), 6.99–6.96 (m, 3H), 6.89–6.85 (m, 3H), 6.71–6.70 (m, 1H), 6.64 (d, 1H, J = 7.5 Hz), 6.59 (d, 1H, J = 8.5 Hz), 6.14–6.12 (m, 1H), 5.33–5.28 (m, 1H), 5.15–5.09 (m, 1H), 4.47–4.41 (m, 1H), 4.36–4.32 (m, 1H), 4.20–4.17 (m, 1H), 3.98–3.95 (m, 1H), 3.85 (s, 3H), 3.31 (m, 1H), 3.18–3.15 (m, 1H), 3.08–3.01 (m, 2H), 2.92–2.88 (m, 1H), 2.53–2.45 (m, 1H), 2.42–2.40 (m, 1H), 2.30–2.26 (m, 2H), 1.93–1.89 (m, 2H), 1.76–1.73 (m, 1H), 1.38–1.33 (m, 1H), 0.95 (s, 3H), 0.91 (s, 3H); ^{13}C-NMR (125 MHz, $CDCl_3$) δ 170.5, 163.2, 158.6, 154.5, 138.7, 133.1, 129.6, 129.5, 126.7, 126.3, 125.5, 118.1, 116.3, 114.5, 73.6, 66.6, 58.9, 55.7, 53.9, 53.8, 35.8, 34.5, 34.5, 32.2, 27.3, 20.2, 19.9; HRMS m/z $(M + Na)^+$ calcd for $C_{34}H_{42}N_2O_7SNa$ 645.2610, found 645.2622.

(2′*R*,3″*S*)-*N*-[2′-Hydroxy-2-(10-hydroxy-5-oxo-19-oxa-4-aza-tricyclo[18.2.2.06,11]tetracosa-1(23),6,8,10,14,20(24),21-heptaen-3″-yl)-ethyl]-*N*-isobutyl-4-methoxy-benzenesulfonamide (8c)

To a solution of diene **7c** (12.4 mg, 0.0187 mmol) and dry DCM (5 mL) was added Grubbs' first generation catalyst (1.2 mg) and the reaction was stirred for 4 hours, and then concentrated under reduced pressure. Flash column chromatography (30–40% EtOAc–hexanes) afforded olefin **8c** (10.5 mg, 85% yield) as a 5 : 1 (by ^{1}H-NMR analysis) mixture of inseparable isomers. ^{1}H-NMR (500 MHz, $CDCl_3$) δ 7.76 (dd, 2H, J = 2.0, 7.0 Hz), 7.08 (d, 2H, J = 8.5 Hz), 7.02–6.99 (m, 3H), 6.81 (d, 2H, J = 8.5 Hz), 6.75–6.07 (m, 2H), 5.86 (d, 1H, J = 9.5 Hz), 5.32 (bs, 1H), 5.26–5.20 (m, 1H), 5.12–5.06 (m, 1H), 4.35–4.29 (m, 1H), 4.14–4.11 (m, 1H), 3.98–3.92 (m, 2H), 3.87 (s, 3H), 3.82–3.77 (bs, 1H), 3.30 (dd, 1H, J = 9.0, 15.0 Hz), 3.14 (dd, 2H, J = 2.5, 15.0 Hz), 3.07 (dd, 1H, J = 3.5, 13.0 Hz), 2.90 (dd, 1H, J = 6.5, 13.5 Hz), 2.52–2.47 (m, 1H), 2.36–2.28 (m, 1H), 2.19–2.11 (m, 2H), 2.07–2.00 (m, 1H), 1.97–1.91 (m, 1H), 1.75–1.55 (m, 3H), 1.41–1.35 (m, 1H), 0.99 (d, 3H, J = 6.5 Hz), 0.94 (d, 3H, J = 6.5 Hz); ^{13}C-NMR (125 MHz, $CDCl_3$) δ 169.9, 163.2, 158.9, 154.3, 138.5, 134.0, 130.1, 129.6, 127.3, 126.9, 125.9, 118.4, 116.5, 115.4, 114.5, 73.6, 66.6, 59.2, 55.7, 54.7,

54.0, 35.1, 32.0, 29.7, 29.4, 28.3, 27.7, 27.4, 20.2, 19.9; HRMS *m/z* (M + Na)$^+$ calcd for $C_{35}H_{44}N_2O_7SNa$ 659.2767, found 659.2766.

(2′*R*,3″*S*)-*N*-[2′-Hydroxy-2-(10-hydroxy-5-oxo-20-oxa-4-aza-tricyclo[19.2.2.06,11]pentacosa-1(24),6,8,10,14,21(25),22-heptaen-3″-yl)-ethyl]-*N*-isobutyl-4-methoxy-benzenesulfonamide (8d)

To diene **7d** (12.8 mg, 0.019 mmol) and dry DCM (4 mL) was added Grubbs' first generation catalyst (1.2 mg). The solution was stirred for 4 hours at room temperature, and then concentrated under reduced pressure. Flash column chromatography (25–40% EtOAc–hexanes) afforded olefin **8d** (10.7 mg, 87% yield) as a single (by ^{1}H-NMR analysis) isomer. ^{1}H-NMR (500 MHz, $CDCl_3$) δ 7.76 (dd, 2H, J = 2.0, 7.0 Hz), 7.10 (d, 2H, J = 8.5), 7.04–6.98 (m, 3H), 6.82–6.76 (m, 4H), 5.94 (d, 1H, J = 10.0 Hz), 5.30–5.22 (m, 3H), 4.36–4.33 (m, 1H), 4.15–4.06 (m, 2H), 3.98–3.95 (m, 1H), 3.87 (s, 3H), 3.82–3.80 (bs, 1H), 3.31 (dd, 1H, J = 9.0, 15.5 Hz), 3.20–3.04 (m, 3H), 2.89 (dd, 1H, J = 6.5, 13.5 Hz), 2.53 (t, 1H, J = 13.0 Hz), 2.38 (dt, 1H, J = 3.5, 11.5 Hz), 2.09–2.05 (m, 2H), 1.95–1.77 (m, 6H); ^{13}C-NMR (125 MHz, $CDCl_3$) δ 169.9, 163.2, 156.9, 154.1, 138.3, 130.7, 130.0, 129.9, 129.6, 129.5, 126.9, 126.4, 118.7, 116.7, 115.2, 114.5, 73.7, 67.1, 59.2, 55.7, 54.3, 54.1, 34.9, 32.7, 30.9, 27.9, 27.4, 26.5, 24.0, 20.2, 19.9; HRMS *m/z* (M + H)$^+$ calcd for $C_{34}H_{46}N_2O_7SNa$ 673.2923, found 673.2921.

Inhibitor 23 and saturated inhibitor 24a

To a stirred solution of olefin **8a** (9 mg, 0.02 mmol) in 5 mL of 1% NH_3 in MeOH solution, 5% Pd/C (1 mg) was added, and the resulting suspension was stirred at 23 °C under a hydrogen filled balloon for 4 h. The mixture was filtered through Celite and concentrated. Silica gel chromatography (40% EtOAc–hexanes) afforded the ring-opened acyclic product **23** (2.5 mg, 27% yield) and saturated macrocycle **24a** (3.6 mg, 40% yield).

Compound 23

^{1}H NMR (500 MHz, $CDCl_3$): δ 7.70 (d, 2H, J = 9 Hz), 7.14 (d, 2H, J = 8.5 Hz), 6.99–6.96 (m, 3H), 6.78–6.75 (m, 3H), 6.56 (d, 1H, J = 7.5 Hz), 5.99 (d, 1H, J = 8.5 Hz), 5.21 (bs, 1H), 5.09 (bs, 1H), 4.32–4.29 (m, 1H), 4.20 (m, 1H), 3.97–3.96 (m, 1H), 3.87 (s, 3H), 3.15–3.02 (m, 3H), 2.98–2.82 (m, 3H), 2.56–2.47 (m, 2H), 1.91–1.88 (m, 1H), 1.49–1.43 (m, 2H), 1.27–1.24 (m, 3H), 0.93 (d, 3H, J = 7.0 Hz), 0.89 (d, 3H, J = 6.5 Hz), 0.85 (t, 3H, J = 6.5 Hz). ^{13}C NMR (125 MHz, $CDCl_3$): δ 170.5, 163.1, 154.5, 154.1, 137.6, 130.5, 129.8, 129.6, 129.4, 127.2, 126.8, 119.0, 117.0, 115.5, 114.4, 72.9, 58.9, 55.6, 54.3, 53.7, 34.0, 32.1, 29.9, 29.7, 27.4, 26.9, 22.5, 20.1, 19.9, 14.0. LRMS-ESI (*m/z*): 635.6 (M + Na)$^+$; HRMS *m/z* (M + H)$^+$ calcd for $C_{33}H_{44}N_2O_7SH$ 613.2947, found 613.2955.

Saturated macrocycle 24a

^{1}H NMR (500 MHz, $CDCl_3$): δ 7.76 (d, 2H, J = 9.0 Hz), 7.23 (d, 1H, J = 9.5 Hz), 7.045–7.015 (m, 2H), 6.99 (d, 2H, J = 9 Hz), 6.91 (d, 1H, J = 8 Hz), 6.82 (d, 2H, J = 9.5 Hz), 6.77 (d, 1H, J = 8 Hz), 5.80 (d, 1H, J = 9.5 Hz), 4.89 (s, 1H), 4.30–4.26 (m, 2H), 4.15–4.11 (m, 1H), 3.95 (m, 1H), 3.86 (s, 3H), 3.72 (d, 1H, J = 2 Hz), 3.28–3.22 (m, 2H), 3.12–3.04 (m, 3H), 2.86 (dd, 1H, J = 6.5, 13.5 Hz), 2.59–2.53 (m, 2H), 2.24 (td, 1H, J = 4.0, 12.8 Hz), 2.01–1.96 (m, 1H), 1.94–1.90 (m, 1H), 1.27–1.245 (m, 3H), 0.99 (d, 3H, J = 6.5 Hz), 0.93 (d, 3H, J = 7.0 Hz). ^{13}C NMR (125 MHz, $CDCl_3$): δ 169.4, 163.1, 159.5, 154.8, 137.0, 130.8, 130.5, 129.5, 129.1, 127.8, 126.6, 119.7, 119.2, 117.3, 117.1, 114.5, 73.8, 69.5, 59.2, 55.6, 54.1, 53.8, 34.8, 30.8, 27.9, 27.4, 26.9, 26.0, 20.2, 19.9. LRMS-ESI *m/z*: 633.5 (M + Na)$^+$; HRMS *m/z* (M + Na)$^+$ calc'd for $C_{33}H_{42}N_2O_7SNa$ 633.2610, found 633.2631.

Saturated inhibitor 24b

Olefin **8b** (3.5 mg), EtOAc (2 mL), and 10% Pd/C (0.5 mg) were stirred under a hydrogen atmosphere for 2 hours. The reaction mixture was filtered through Celite and concentrated. Flash column chromatography (30% EtOAc–hexanes) afforded saturated macrocycle **24b** (3.3 mg, 94% yield). ^{1}H-NMR (500 MHz, $CDCl_3$) δ 7.75 (td, 2H, J = 3.0, 9.0), 7.13–7.05 (m, 1H), 6.98 (td, 2H, J = 2.0, 9.0 Hz), 6.92 (t, 1H, J = 7.5 Hz), 6.88 (d, 2H, J = 6.0 Hz), 6.71 (d, 2H, J = 9.0 Hz), 6.10 (bs, 1H), 6.04 (d, 1H, J = 9.5 Hz), 4.40–4.37 (m, 1H), 4.33–4.29 (m, 1H), 4.22 (td, 1H, J = 4.0, 12.0 Hz), 4.00–3.96 (m, 1H), 3.85 (s, 3H), 3.30 (dd, 1H, J = 9.0, 15.0 Hz), 3.16–3.11 (m, 2H), 3.05 (dd, 1H, J = 8.5, 13.0 Hz), 2.89 (dd, 1H, J = 6.5, 13.5 Hz), 2.57–2.51 (m, 1H), 2.38 (dt, 1H, J = 4.0, 13.0 Hz), 1.94–1.90 (m, 1H), 1.80–1.72 (m, 2H), 1.49–1.40 (m, 2H), 1.30–1.22 (m, 2H), 1.20–1.12 (m, 3H), 0.97 (d, 3H, J = 6.5 Hz), 0.92 (d, 3H, J = 6.5 Hz); ^{13}C-NMR (125 MHz, $CDCl_3$) δ 170.1, 163.2, 158.0, 154.6, 137.7, 130.3, 130.2, 129.6, 129.5, 127.7, 126.5, 118.6, 117.2, 116.8, 114.5, 73.7, 68.2, 59.1, 55.7, 54.1, 53.9, 34.6, 29.1, 28.1, 27.4, 26.8, 24.0, 20.2, 19.9; HRMS *m/z* (M + Na)$^+$ calcd for $C_{34}H_{44}N_2O_7SNa$ 647.2767, found 647.2761.

Saturated inhibitor 24c

Olefin **8c** (4.0 mg, 0.0063 mmol) was dissolved in ethyl acetate (5 mL) and 10% Pd/C (1 mg) was added. The mixture was stirred under a hydrogen atmosphere for 4 hours and then filtered through Celite. After concentration under reduced pressure, the product was purified by flash column chromatography (30% EtOAc–hexanes) to afford the macrocycle **24c** (3.5 mg, 88% yield). ^{1}H-NMR (500 MHz, $CDCl_3$) δ 7.76 (ddd, 2H, J = 2.0, 3.0, 9.0 Hz), 7.09–7.04 (m, 3H), 6.99 (ddd, 2H, J = 2.0, 3.0, 9.0 Hz), 6.87 (dd, 1H, J = 1.0, 7.5 Hz), 6.82 (d, 2H, J = 8.5 Hz), 6.80 (dd, 1H, J = 1.0, 8.0 Hz), 5.90 (d, 1H, J = 9.0 Hz), 4.91 (bs, 1H), 4.37 (dt, 1H, J = 4.0, 12.0 Hz), 4.28–4.23 (m, 1H), 4.17–4.13 (m, 1H), 3.98–3.95 (m, 1H), 3.86 (s, 3H), 3.30 (dd, 1H, J = 9.0, 15.5 Hz), 3.17–3.13 (m, 2H), 3.06 (dd, 1H, J = 8.6, 13.0 Hz), 2.87 (dd, 1H, J = 6.5, 13.5 Hz), 2.71–2.65 (m, 1H), 2.60 (dd, 1H, J = 12.0, 14.5 Hz), 2.03–1.97 (m, 1H), 1.96–1.90 (m, 2H), 1.62–1.55 (m, 3H), 1.45–1.42 (m, 2H), 1.39–1.34 (m, 1H), 1.05–1.01 (m, 3H), 0.98 (d, 3H, J = 6.5 Hz), 0.92 (d, 3H, J = 6.5 Hz); ^{13}C-NMR (125 MHz, $CDCl_3$) δ 170.1, 163.1, 156.9, 154.3, 137.3, 130.1, 129.7, 129.7, 129.5, 127.5, 126.7, 119.2, 117.1, 115.8, 114.5, 73.6, 68.0, 59.2, 55.7, 55.0, 54.0, 34.9, 29.7, 29.4, 28.9, 27.6, 27.4, 26.7, 26.1, 25.4, 20.2, 19.9; HRMS *m/z* (M + Na)$^+$ calcd for $C_{35}H_{46}N_2O_7SNa$ 661.2923, found 661.2921.

This journal is © The Royal Society of Chemistry 2014

Saturated inhibitor 24d

Olefin **8d** (4.5 mg, 0.0069 mmol) was dissolved in EtOAc (3 mL) and 10% Pd/C (0.5 mg) was added. The mixture was stirred under a H_2 atmosphere for 4 hours, then filtered through Celite and concentrated under reduced pressure. Flash column chromatography (40% EtOAc–hexanes) afforded a saturated macrocycle **24d** (4.0 mg, 89% yield). ^{1}H-NMR (500 MHz, $CDCl_3$) δ 7.75 (ddd, 2H, J = 2.0, 2.5, 9.0 Hz), 7.12 (d, 2H, J = 8.5 Hz), 7.03 (t, 1H, J = 8.0 Hz), 7.00 (ddd, 2H, J = 3.0, 4.0, 9.0 Hz), 6.82 (d, 2H, J = 9.0 Hz), 6.80–6.76 (m, 2H), 5.94 (d, 1H, J = 9.5 Hz), 5.05 (bs, 1H), 4.40–4.34 (m, 1H), 4.18–4.12 (m, 2H), 3.99–3.95 (m, 1H), 3.87 (s, 3H), 3.31 (dd, 1H, J = 9.0, 15.0 Hz), 3.15–3.11 (m, 2H), 3.07 (dd, 1H, J = 9.0, 13.5 Hz), 2.88 (dd, 1H, J = 6.5, 13.5 Hz), 2.59 (dd, 1H, J = 12.0, 14.5 Hz), 2.50 (dt, 1H, J = 3.5, 12.5 Hz), 1.96–1.90 (m, 1H), 1.90–1.82 (m, 1H), 1.75–1.71 (m, 1H), 1.65–1.54 (m, 4H), 1.50–1.44 (m, 1H), 1.36–1.33 (m, 2H), 1.10–1.03 (m, 4H), 0.99 (d, 3H, J = 6.5 Hz), 0.93 (d, 3H, J = 6.5 Hz); ^{13}C-NMR (125 MHz, $CDCl_3$) δ 170.1, 163.2, 156.8, 154.1, 138.0, 129.9, 129.6, 129.6, 129.5, 127.1, 126.7, 119.0, 116.8, 115.1, 114.5, 73.7, 67.0, 59.2, 55.7, 54.2, 54.0, 34.7, 30.0, 29.7, 28.3, 27.4, 27.1, 27.0, 26.8, 26.2, 23.0, 20.2, 19.9; HRMS m/z $(M + Na)^+$ calcd for $C_{36}H_{48}N_2O_7SNa$ 675.3080, found 675.3086.

Acknowledgements

Financial support for this work was provided by the National Institute of Health (GM 53386). This work was also supported by the Intramural Research Program of the Center for Cancer Research, National Cancer Institute, National Institutes of Health and in part by a Grant-in-aid for Scientific Research (Priority Areas) from the Ministry of Education, Culture, Sports, Science, and Technology of Japan (Monbu Kagakusho), a Grant for Promotion of AIDS Research from the Ministry of Health, Welfare, and Labor of Japan (Kosei Rohdosho: H15-AIDS-001), and the Grant to the Cooperative Research Project on Clinical and Epidemiological Studies of Emerging and Re-emerging Infectious Diseases (Renkei Jigyo: No. 78, Kumamoto University) of Monbu-Kagakusho. We would like to thank Dr Kalapala Venkateswara Rao (Purdue University) for helpful discussions.

References

1 S. Hue, R. J. Gifford, D. Dunn, E. Fernhill and D. Pillay, *J. Virol.*, 2009, **83**, 2645–2654.
2 B. Conway, *Future Virol.*, 2009, **4**, 39–41.
3 R. Gupta, A. Hill, A. W. Sawyer and D. Pillay, *Clin. Infect. Dis.*, 2008, **47**, 712–722.
4 M. A. Wainberg and G. Friedland, *J. Med. Chem. Assoc.*, 1998, **279**, 1977–1983.
5 A. K. Ghosh, Z. L. Dawson and H. Mitsuya, *Bioorg. Med. Chem. Lett.*, 2007, **15**, 7576–7580.
6 A. K. Ghosh, B. D. Chapsal, I. T. Weber and H. Mitsuya, *Acc. Chem. Res.*, 2008, **41**, 78–86.
7 Y. Koh, H. Nakata, K. Maeda, H. Ogata, G. Bilcer, T. Devasamudram, J. F. Kincaid, P. Boross, Y. F. Wang, Y. Tie, P. Volarath, L. Gaddis, R. W. Harrison, I. T. Weber, A. K. Ghosh and H. Mitsuya, *Antimicrob. Agents Chemother.*, 2003, **47**, 3123–3129.
8 A. K. Ghosh, D. D. Anderson, I. T. Weber and H. Mitsuya, *Angew. Chem., Int. Ed.*, 2012, **51**, 1778–1802.
9 A. K. Ghosh, S. Kulkarni, D. D. Anderson, L. Hong, A. Baldridge, Y. F. Wang, A. A. Chumanevich, A. Y. Kovalevsky, Y. Tojo, M. Amano, Y. Koh, J. Tang, I. T. Weber and H. Mitsuya, *J. Med. Chem.*, 2009, **52**, 7689–7705.
10 A. K. Ghosh, L. Swanson, C. Liu, H. Cho, A. Hussain, D. E. Walters and L. Holland, *Bioorg. Med. Chem. Lett.*, 2002, **12**, 1993–1996.
11 A. K. Ghosh, L. M. Swanson, H. Cho, S. Leshchenko, K. A. Hussain, S. Kay, D. E. Walters, Y. Koh and H. Mitsuya, *J. Med. Chem.*, 2005, **48**, 3576–3585.
12 D. J. Kempf, K. C. Marsh, D. A. Paul, M. F. Knigge, D. W. Norbeck, W. E. Kohlbrenner, L. Codacovi, S. Vasavanonda, P. Bryant, X. C. Wang, N. E. Wideburg, J. J. Clement, J. J. Plattner and J. Erickson, *Antimicrob. Agents Chemother.*, 1991, **35**, 2209–2214.
13 E. T. Baldwin, T. N. Bhat, B. Liu, N. Pattabiraman and J. W. Erickson, *Nat. Struct. Biol.*, 1995, **2**, 244–249.
14 R. C. Reid, L. K. Pattenden, J. D. A. Tyndall, J. L. Martin, T. Walsh and D. P. Fairlie, *J. Med. Chem.*, 2004, **47**, 1641–1651.
15 K. Yoshimura, R. Kato, M. F. Kavlick, A. Nguyen, V. Maroun, K. Maeda, K. A. Hussain, A. K. Ghosh, S. V. Gulnik, J. W. Erickson and H. Mitsuya, *J. Virol.*, 2002, **76**, 1349–1358.
16 S. W. Kaldor, V. J. Kalish, J. F. Davies 2nd, B. V. Shetty, J. E. Fritz, K. Appelt, J. A. Burgess, K. M. Campanale, N. Y. Chirgadze, D. K. Clawson, B. A. Dressman, S. D. Hatch, D. A. Khalil, M. B. Kosa, P. P. Lubbehusen, M. A. Muesing, A. K. Patick, S. H. Reich, K. S. Su and J. H. Tatlock, *J. Med. Chem.*, 1997, **40**, 3979–3985.
17 M. Kozisek, J. Bray, P. Rezacova, K. Saskova, J. Brynda, J. Pokorna, F. Mammano, L. Rulisek and J. Konvalinka, *J. Mol. Biol.*, 2007, **374**, 1005–1016.
18 A. K. Ghosh, W. J. Thompson, M. K. Holloway, S. P. McKee, T. T. Duong, H. Y. Lee, P. M. Munson, A. M. Smith, J. M. Wai and P. L. Darke, *J. Med. Chem.*, 1993, **36**, 2300–2310.
19 R. A. Fernandes, M. S. Bodas and P. Kumar, *Tetrahedron*, 2002, **58**, 1223–1227.
20 Y. Gao, R. M. Hanson, J. M. Klunder, S. Y. Ko, H. Masamune and K. B. Sharpless, *J. Am. Chem. Soc.*, 1987, **109**, 5765–5780.
21 M. Caron, K. Carlier and K. B. Sharpless, *J. Org. Chem.*, 1988, **53**, 5185–5187.
22 A. K. Ghosh, S. P. McKee, H. Y. Lee and W. T. Thompson, *J. Chem. Soc., Chem. Commun.*, 1992, 273–274.

23 A. K. Ghosh, P. R. Sridhar, S. Leshchenko, A. K. Hussain, J. Li, A. Y. Kovalevsky, D. E. Walters, J. E. Wedekind, V. Grum-Tokars, D. Das, Y. Koh, K. Maeda, H. Gatanaga, I. T. Weber and H. Mitsuya, *J. Med. Chem.*, 2006, **49**, 5252–5261.
24 R. F. Hudson and P. A. Chopard, *Helv. Chim. Acta*, 1963, **46**, 2178.
25 S. Doulut, I. Dubuc, M. Rodriguez, F. Vecchini, H. Fulcrand, F. Barelli, E. Checler, E. Bourdel and A. Aumeles, *J. Med. Chem.*, 1993, **36**, 1369–1379.
26 R. Bacaloglu, A. Blasko, C. A. Bunton, G. Cerichelli, F. Castaneda and E. Rivera, *J. Chem. Soc., Perkin Trans. 2*, 1995, 965–972.
27 T. K. Jones and S. E. Denmark, *Org. Synth.*, 1990, 524, *Coll. Vol. VII.*
28 R. Ostwald, P.-Y. Chavant, H. Stadtmüller and P. Knochel, *J. Org. Chem.*, 1994, **59**, 4143–4153.
29 S. Serra, C. Fuganti and A. Moro, *J. Org. Chem.*, 2001, **66**, 7883–7888.
30 E. Brenna, C. Fuganti, V. Perozzo and S. Serra, *Tetrahedron*, 1997, **53**, 15029–15040.
31 P. Schwab, M. B. France, J. W. Ziller and R. C. Grubbs, *Angew. Chem., Int. Ed. Engl.*, 1995, **34**, 2039–2041.
32 M. S. Sanford, J. A. Love and R. H. Grubbs, *J. Am. Chem. Soc.*, 2001, **123**, 6543–6554.
33 H. Sajiki and K. Hirota, *Tetrahedron*, 1998, **54**, 13981–13996.
34 M. V. Toth and G. R. Marshall, *Int. J. Pept. Protein Res.*, 1990, **36**, 544–550.
35 M. Amano, Y. Koh, D. Das, Y.-F. Wang, P. I. Boross, J. Li, S. Leschenko, I. T. Weber, A. K. Ghosh and H. Mitsuya, *Antimicrob. Agents Chemother.*, 2007, **51**, 2143–2155.
36 Y. Tie, P. I. Boross, Y. F. Wang, L. Gaddis, A. K. Hussain, S. Leshchenko, A. K. Ghosh, J. M. Louis, R. W. Harrison and I. T. Weber, *J. Mol. Biol.*, 2004, **338**, 341–352.

This journal is © The Royal Society of Chemistry 2014

Journal of Cardiology Cases 10 (2014) 167–170

Contents lists available at ScienceDirect

Journal of Cardiology Cases

journal homepage: www.elsevier.com/locate/jccase

Case Report

A case of human immunodeficiency virus-related heart failure resembling dilated cardiomyopathy but accompanied by high cardiac output

Noriaki Tabata (MD)[a,1], Megumi Yamamuro (MD, PhD)[a,1], Seigo Sugiyama (MD, PhD, FJCC)[a,*], Michio Mizobe (MD)[a], Seiji Takashio (MD, PhD)[a], Kenichi Tsujita (MD, PhD)[a], Eiichiro Yamamoto (MD, PhD)[a], Tomoko Tanaka (MD, PhD)[a], Sunao Kojima (MD, PhD, FJCC)[a], Koichi Kaikita (MD, PhD, FJCC)[a], Shinji Tayama (MD, PhD)[a], Seiji Hokimoto (MD, PhD, FJCC)[a], Chiharu Syudo (MD)[b], Toshikazu Miyakawa (MD, PhD)[b], Hiroaki Mitsuya (MD, PhD)[b], Hisao Ogawa (MD, PhD, FJCC)[a]

[a] *Department of Cardiovascular Medicine, Graduate School of Medical Sciences, Kumamoto University, Kumamoto City, Japan*
[b] *Department of Infectious Diseases and Hematology, Kumamoto University Graduate School of Medical Sciences, Kumamoto City, Japan*

ARTICLE INFO

Article history:
Received 24 February 2014
Received in revised form 8 June 2014
Accepted 13 June 2014

Keywords:
Heart failure
Cardiomyopathy
Human immunodeficiency virus
High cardiac output

ABSTRACT

A 34-year-old man presented with heart failure (HF). He suffered opportunistic infections and was shown to be human immunodeficiency virus (HIV)-positive (viral load: 156,013 copies/mL) and have low CD4 lymphocytes (3/mm^3), so he was initially treated for the opportunistic infections. Initial investigations showed high elevation of brain natriuretic peptide (BNP: 969 pg/mL). Transthoracic echocardiography showed an enlarged left ventricle (LV: 70 mm), a reduced LV ejection fraction (EF: 19%), but no LV hypertrophy or significant valvular diseases. After treatments for the infections, we started standard HF medications. Cardiac catheterization, after recovery from the opportunistic infections with negative inflammatory markers, showed no significant coronary stenosis, and endomyocardial biopsy did not show findings of myocarditis, without HIV structural protein on immunohistochemistry. Despite reduced EF, the cardiac output was elevated at 7.1 l/min [cardiac index (CI): 4.3 l/min/m^2] and the systemic vascular resistance index was decreased at 1358 dynes s/cm^5 m^2. Hematologists began anti-retroviral therapy; the viral load was gradually reduced to negative, and the CD4 count was increased to 50/mm^3 at Day 182. EF was accordingly improved up to 54%, but the cardiac output decreased to a normal level at 3.9 l/min (CI: 2.4 l/min/m^2), leading to normalization of plasma BNP (<5 pg/mL). This case indicates that high cardiac output might be involved in the pathogenic mechanisms of HIV-related HF.

<**Learning objective:** The etiology of HIV-related HF remains unclarified. We report on a man with HIV-associated HF. There were no apparent causes of the HF, but the patient did demonstrate high cardiac output despite impaired systolic function. After anti-retroviral therapy, his systolic function was improved with a reduction and normalization of cardiac output. Therefore, this case indicates that high cardiac output might be involved in the pathogenic mechanisms of HIV-related HF.>

© 2014 Japanese College of Cardiology. Published by Elsevier Ltd. All rights reserved.

Introduction

Heart failure associated with human immunodeficiency virus (HIV) was recognized early in the epidemic. HIV-associated myocarditis, nutrition deficiencies including of selenium, drug cardiotoxicity, and inflammatory cytokinemia have been suggested as possible causes; however, the precise etiology of HIV-related heart failure remains unclarified. We report on an HIV-infected man with heart failure. He did not have any of the causative factors described above, but did demonstrate high cardiac output despite impaired systolic left ventricular (LV) function. After anti-retroviral therapy, his LV function improved, with a reduction and normalization of cardiac output. This case indicates that high cardiac output might be involved in the pathogenic mechanisms of HIV-related heart failure.

* Corresponding author at: Department of Cardiovascular Medicine, Graduate School of Medical Sciences, Kumamoto University, 1-1-1 Honjo, Chuo-ku, Kumamoto City 860-8556, Japan. Tel.: +81 96 373 5175; fax: +81 96 362 3256.
E-mail address: ssugiyam@kumamoto-u.ac.jp (S. Sugiyama).
[1] Noriaki Tabata and Megumi Yamamuro contributed equally to this work.

http://dx.doi.org/10.1016/j.jccase.2014.06.006
1878-5409/© 2014 Japanese College of Cardiology. Published by Elsevier Ltd. All rights reserved.

Case report

In October 2011, a 34-year-old man presented at the Hematology Department with HIV infection accompanied by congestive heart failure. In September 2011, he had begun to experience exertional fatigue and was admitted to another hospital because of a fever of unknown origin. He presented with infections of *Pneumocystis jirovecii* and cytomegalovirus with HIV-positivity (viral load: 156,013 copies/mL) and low CD4 lymphocytes (3/mm^3). Blood culture at the previous hospital had not demonstrated sepsis. He was initially treated with trimethoprim-sulfamethoxazole and ganciclovir, and had been recovering from the pulmonary infections. After successful treatment of the opportunistic infections (pneumonia) for one week, he was transferred to our hospital. His past medical history did not reveal any cardiovascular diseases and he had not taken medications for them.

After admission to our hospital, he was referred to the Cardiovascular Medicine Department because he had heart failure, even after one month of recovery from the opportunistic infections (pneumonia). On physical examination, his blood pressure was 104/82 mmHg and his pulse rate was 107 beats/min, with New York Heart Association Classification-II. He had S3 and S4 gallops without significant murmur. There were no rales on the lung and no edema of the extremities. Initial investigations showed high elevation of brain natriuretic peptide (BNP) at 969.2 pg/mL. Renal, liver, and thyroid function test results were all normal, without significant anemia, cytokinemia, or nutrient deficiency including of selenium. A chest radiograph showed heart enlargement and slight pulmonary congestion (Fig. 1A). An electrocardiogram indicated a negative T-wave in V_{4-6} leads and a QS pattern in V_{1-2} leads (Fig. 1B). Transthoracic echocardiography showed an enlarged LV (LV end-diastolic diameter of 70 mm, LV end-systolic diameter of 64 mm) and a reduced LV ejection fraction (EF) of 19%, without LV hypertrophy or significant valvular diseases (Fig. 1C); these findings were compatible with dilated cardiomyopathy. Magnetic resonance imaging demonstrated no late gadolinium enhancement. After treatments of the opportunistic infections, C-reactive

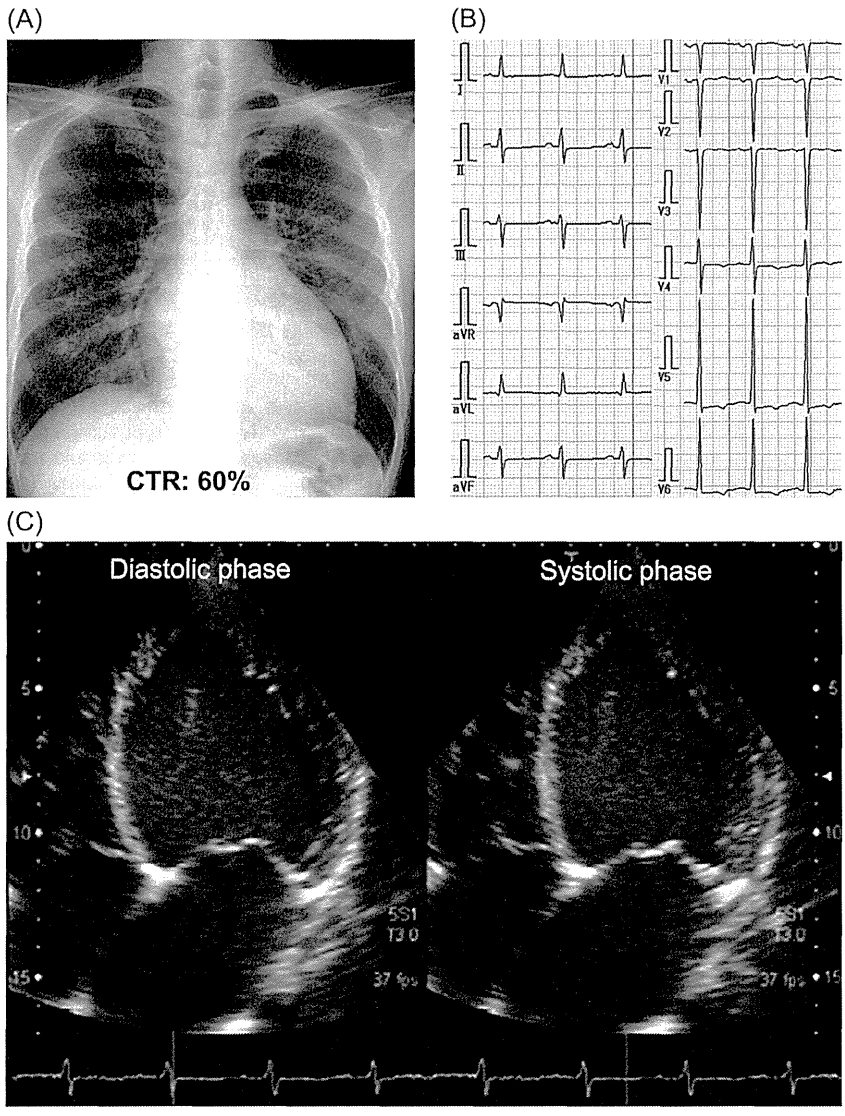

Fig. 1. (A) Chest radiograph of this patient on admission, showing enlarged heart and bilateral infiltrates. (B) Twelve-lead electrocardiogram recorded on admission; sinus tachycardia, mild left axis deviation, negative T-wave in V_{4-6} leads, and QS pattern in V_{1-2} leads were observed. (C) Transthoracic echocardiography, showing enlarged left ventricle and reduced left ventricular ejection fraction (19%), without left ventricular hypertrophy or significant valvular diseases, which was compatible with dilated cardiomyopathy. CTR, cardiothoracic ratio; LVDd, left ventricular end-diastolic diameter; LVEF, left ventricular ejection fraction.

(A)

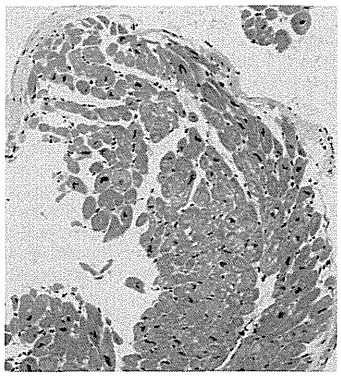

(B)

	pre-cART	post-cART
BT(°C)	36.6	36.4
HR (beats/min)	70	66
BP (mmHg)	96/60	124/68
WBC (/ μL)	5300	3400
Hb (g/dL)	12.1	14.3
CRP (mg/dL)	0.03	0.08
viral load (copies/mL)	156,013	negative
CD4 cell (counts/mm^3)	3	50
LVEF (%)	34	54
CI (l/min/mm^3)	4.3	2.4
SVRI (dines.sec/cm^5m^2)	1358	2723
BNP (pg/mL)	239	<5

Fig. 2. (A) Endomyocardial biopsy showed cardiomyocyte hypertrophy, but no significant cell death or myocarditis. (B) Parameters of this patient before and after (day 182) cART treatment. cART, combination antiretroviral therapy; BT, body temperature; HR, heart rate; BP, blood pressure; WBC, white blood cells; Hb, hemoglobin; CRP, C-reactive protein; LVEF, left ventricular ejection fraction; CI, cardiac index; SVRI, systemic vascular resistance index; BNP, brain natriuretic peptide.

protein (CRP) levels decreased to normal. We started standard heart failure medications consisting of a beta-blocker, angiotensin-converting enzyme inhibitor, an anti-aldosterone agent, and diuretics.

On Day 33, with the patient in a stable condition after recovery from the opportunistic infections with negative CRP, we performed cardiac catheterization. Coronary angiography showed no significant stenosis. Endomyocardial biopsy showed cardiomyocyte hypertrophy but no significant cell death or myocarditis (Fig. 2A). Cytomegalovirus and p24 protein, which is an HIV structural protein, were negative on immunohistochemistry. The LV was still dilated with reduced EF of 39%, but the cardiac output was paradoxically elevated at 7.1 l/min [cardiac index (CI): 4.3 l/min/m^2] and the systemic vascular resistance index (SVRI) was decreased at 1358 dynes s/cm^5 m^2 (LV end-diastolic diameter: 64.7 mm, LV end-systolic diameter: 55.5 mm, LV end-diastolic volume: 229.7 mL, LV end-systolic volume: 139.6 mL, stroke volume: 90 mL, heart rate: 78/min, body surface area: 1.66 m^2). After cardiac catheterization, hematologists began highly active combination antiretroviral therapy (cART) with raltegravir, darunavir, and ritonavir. After cART, the viral load was gradually reduced to negative and the CD4 count was increased to 50/mm^3 at Day 182. LVEF was accordingly improved up to 54%, but the cardiac output was decreased to a normal level of 3.9 l/min (CI: 2.4 l/min/m^2), leading to normalization of plasma BNP (<5 pg/mL) (Fig. 2B). With no side effects of the cART, the patient was discharged and followed up at both hematologic and cardiovascular outpatient clinics.

Discussion

Myocardial diseases associated with HIV were recognized early in the epidemic [1]. As the HIV-infected population ages, heart failure prevalence and mortality including cardiac sudden death are increasing [2]. It was suggested that echocardiographic abnormalities were frequently observed in HIV-positive patients [3]. HIV-associated myocarditis, selenium deficiency, cardiotoxicity from drugs [4], inflammatory cytokinemia, and nutritional deficiencies have been suggested as possible causes of HIV-related heart failure [5]; however, the precise mechanisms and pathogenesis remain unresolved.

Our patient presented with heart failure-like dilated cardiomyopathy with HIV-positivity at the stage of acquired immunodeficiency syndrome (AIDS). He did not have any of the above causative conditions, but showed HIV viremia with significantly elevated virus copy number. Myocardial dysfunction is often a complication in patients with sepsis [6] and we could not rule out the possible involvement of sepsis-associated myocardial dysfunction in the present case. However, our case had opportunistic infections: pneumonia at a previous hospital one week before admission to our hospital, but he did not have sepsis. After successful treatment of the infections, his condition became stable upon admission to our hospital. On the 42nd day from the initial pulmonary infection, clinical examinations at the time of cardiac catheterization before the initiation of cART did not show any findings of inflammation, namely, fever, or the elevation of CRP and white blood cell count. His heart failure was still maintained after optimal heart failure medications and successful recovery from the opportunistic infections before cART. Cardiac catheterization on that occasion demonstrated the presence of high cardiac output and low SVRI, with reduced LVEF. To the best of our knowledge, this is the first report demonstrating that HIV viremia might be one of the causes of high-cardiac-output heart failure. The patient did not have any established causes of high cardiac output: hyperthyroidism, fever, systemic inflammation, dehydration, thiamine deficiency, or anemia [7]. After cART, LVEF and LV were improved, interestingly accompanied by a reduction and normalization of cardiac output. Inflammatory markers (white blood cell count, serum amyloid-A protein, and CRP) were at normal levels, but HIV levels were significantly elevated before cART, so it is possible that the decreased systemic vascular resistance and high cardiac output could have been caused by the high HIV levels, without any clinical evidence of systemic inflammation.

It has been reported that cytokines promote the expression of inducible nitric oxide synthase (iNOS) in cardiomyocytes, inducing myocarditis [8]. However, in this case, endomyocardial biopsy showed no significant cell death or myocarditis. The value of interleukin-6 that we measured was within the normal range (3.9 pg/mL), and we did not measure other cytokines such as tumor necrosis factor-alpha (TNF-alpha) and did not examine iNOS induction in this case. González-Nicolás et al. [9] reported that increased circulating TNF-alpha and nitric oxide (NO) were detected in HIV-infected patients and higher TNF-alpha and NO plasma levels were associated with higher HIV viral load. Therefore, in untreated HIV-infected patients, higher viral load might cause high plasma levels of NO and promote dysregulated vascular tone and uncontrolled vasodilation, decreased systemic vascular resistance, and high cardiac output, resulting in progressive deterioration of cardiac function and heart failure.

It might seem a little strange that this patient had impaired systolic function despite no finding of histological myocardial injury in endomyocardial biopsy. It is possible that the increases in vascular permeability and fluid accumulation might have caused massive elevation of preload, and the enhanced expression of iNOS might have resulted in dilation of the heart.

The accumulation of more cases might confirm our findings.